ARMY RESEARCH LABORATORY

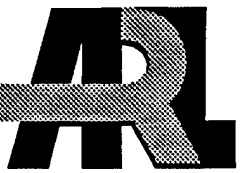

Ab Initio Study of Reactions of *sym*-Triazine

Sharmila V. Pai
Cary F. Chabalowski
Betsy M. Rice

ARL-TR-1096 June 1996

NOTICES

Destroy this report when it is no longer needed. DO NOT return it to the originator.

Additional copies of this report may be obtained from the National Technical Information Service, U.S. Department of Commerce, 5285 Port Royal Road, Springfield, VA 22161.

The findings of this report are not to be construed as an official Department of the Army position, unless so designated by other authorized documents.

The use of trade names or manufacturers' names in this report does not constitute indorsement of any commercial product.

REPORT DOCUMENTATION PAGE

Form Approved
OMB No. 0704-0188

1. AGENCY USE ONLY *(Leave blank)*	2. REPORT DATE	3. REPORT TYPE AND DATES COVERED
	June 1996	Final, Mar 94–Aug 94

4. TITLE AND SUBTITLE

Ab Initio Study of Reactions of *sym*-Triazine

5. FUNDING NUMBERS

1L161102AH43

6. AUTHOR(S)

Sharmila V. Pai, Cary F. Chabalowski, and Betsy M. Rice

7. PERFORMING ORGANIZATION NAME(S) AND ADDRESS(ES)

U.S. Army Research Laboratory
ATTN: AMSRL-WT-PC
Aberdeen Proving Ground, MD 21005-5066

8. PERFORMING ORGANIZATION REPORT NUMBER

ARL-TR-1096

9. SPONSORING/MONITORING AGENCY NAMES(S) AND ADDRESS(ES)

10.SPONSORING/MONITORING AGENCY REPORT NUMBER

11. SUPPLEMENTARY NOTES

12a. DISTRIBUTION/AVAILABILITY STATEMENT

Approved for public release; distribution is unlimited.

12b. DISTRIBUTION CODE

13. ABSTRACT ***(Maximum 200 words)***

Ab initio calculations were performed to investigate reaction mechanisms for formation and decomposition of the six-membered ring $C_3N_3H_3$, known as *sym*-triazine. MP2 geometry optimizations with QCISD(T) energy refinements for critical points on the potential energy surface were calculated with the 6-31G**, 6-311++G**, and cc-pVTZ basis sets. Good agreement is found for MP2 geometries and frequencies of *sym*-triazine and HCN when compared with the corresponding experimental values. Two decomposition mechanisms of *sym*-triazine, the concerted triple dissociation (*sym*-triazine $\rightarrow$ 3 HCN) and the step-wise decomposition (*sym*-triazine $\rightarrow H_2C_2N_2$ + HCN $\rightarrow$ 3 HCN) were investigated. All calculations show that the lowest-energy decomposition mechanism is the concerted triple dissociation. Our best calculations predict the zero-point-energy-corrected barrier to decomposition to be 81.2 kcal/mol. The calculated reaction enthalpy is 35.5 kcal/mol, 7.7 kcal/mol lower than experiment. Intrinsic reaction coordinate (IRC) calculations leading from the transition state of the concerted triple dissociation reaction to three HCN molecules led to a minimum on the potential energy surface. The corresponding structure is a cyclic $(HCN)_3$ cluster. The temperature-corrected formation enthalpy of the cluster is −8.7 kcal/mol relative to three isolated HCN molecules. The zero-point-corrected barrier to formation of *sym*-triazine from the cluster is 58.1 kcal/mol. QCISD(T) energy refinements did not differ significantly from the MP2 results.

14. SUBJECT TERMS

ab initio, *sym*-triazine, potential energy surfaces, intrinsic reaction coordinate (IRC)

15. NUMBER OF PAGES

38

16. PRICE CODE

17. SECURITY CLASSIFICATION OF REPORT	18. SECURITY CLASSIFICATION OF THIS PAGE	19. SECURITY CLASSIFICATION OF ABSTRACT	20. LIMITATION OF ABSTRACT
UNCLASSIFIED	UNCLASSIFIED	UNCLASSIFIED	UL

INTENTIONALLY LEFT BLANK.

ACKNOWLEDGMENTS

This work was supported by the Program Manager, Non-Stockpile Chemical Materiel U.S. Army Chemical Demilitarization and Remediation Activity. The authors thank Dr. Michael McQuaid for helpful discussions.

INTENTIONALLY LEFT BLANK.

TABLE OF CONTENTS

		Page
	ACKNOWLEDGMENTS	iii
	LIST OF FIGURES	vii
	LIST OF TABLES	ix
1.	INTRODUCTION	1
2.	METHODS	3
3.	RESULTS AND DISCUSSION	3
3.1	Geometries	6
3.2	Frequencies	9
3.3	Vibrational Coupling	13
3.4	Energetics	14
4.	CONCLUSIONS	22
5.	REFERENCES	25
	DISTRIBUTION LIST	27

INTENTIONALLY LEFT BLANK.

LIST OF FIGURES

Figure		Page
1.	Structures of (a) *sym*-triazine; (b) transition state for the concerted triple dissociation and association reactions [reactions (I) and (III)]; (c) the stable dimer species $H_2C_2N_2$ associated with the stepwise dissociation mechanism [reaction (II)]; (d) HCN; and (e) the hydrogen-bonded $(HCN)_3$ cluster located on the concerted triple association/dissociation path	4
2.	MP2/6-31G** reaction path from the IRC calculation for reactions (I) and (III). Every tenth point of the IRC is shown	7
3.	Internal coordinate changes along the MP2/6-31G** IRC for the concerted triple association/dissociation reactions	8
4.	MP2/cc-pVTZ vibrational eigenvectors for *sym*-triazine	10
5.	MP2/cc-pVTZ vibrational eigenvectors for the transition state leading to concerted triple dissociation/association of *sym*-triazine [reactions (I) and (III)]	11
6.	MP2/cc-pVTZ vibrational eigenvectors for the $(HCN)_3$ cluster	12
7.	Projection of the eigenvectors corresponding to the MP2/6-31G** harmonic vibrational frequencies of *sym*-triazine onto eigenvectors for points on the reaction path that correspond to the direction along the path for the concerted triple association/decomposition reactions [reactions (I) and (III)]	15
8.	Projection of the eigenvectors corresponding to the MP2/6-31G** harmonic vibrational frequencies of the $(HCN)_3$ cluster onto eigenvectors for points on the reaction path that correspond to the direction along the path for the concerted triple association/decomposition reactions [reactions (I) and (III)]	16
9.	Comparison of MP2 and QCISD(T) (a) barriers to the formation of *sym*-triazine; and (b) barriers to decomposition of *sym*-triazine	19
10.	Schematic of the overall energetics for the reactions 3HCN → *sym*-triazine	21

INTENTIONALLY LEFT BLANK.

LIST OF TABLES

Table		Page
1.	MP2 Optimized Structural Parameters, Harmonic Frequencies, and Zero-Point Energies	5
2.	Absolute Energies (Hartrees) and Relative Energies With and Without Zero-Point Energy (ZPE) Corrections (kcal/mol) of Species on the *sym*-Triazine Potential Energy Surface	18
3.	Temperature-Corrected (T=298 K) Enthalpies (kcal/mol)	20

INTENTIONALLY LEFT BLANK.

1. INTRODUCTION

The chemical simplicity of hydrocyanic acid (HCN) and its multimers makes them attractive candidates for experimental and theoretical study. Due to its extreme toxicity, HCN must be handled with caution. Additionally, HCN is reported to be unstable upon storage with the possibility of explosion due to polymerization, presumably in forming 1,3,5-triazine ($C_3N_3H_3$), also known as *sym*-triazine (Migrdichian 1947). To explore the possibility of high-energy release in the formation of *sym*-triazine from HCN, more information is needed on the reaction mechanism and barrier height to formation. Unfortunately, very little is known about the potential energy surface (PES) for the polymerization of HCN to *sym*-triazine. There have been experimental studies on the reverse reaction, the decomposition of *sym*-triazine to form HCN (Ondrey and Bersohn 1984; Goates, Chu, and Flynn 1984).

$$\textit{sym}\text{-triazine} \rightarrow 3\ \text{HCN} \qquad \Delta H = 43.2\ \text{kcal/mol} \tag{I}$$

Photodissociation experiments at 248 and 193 nm showed that *sym*-triazine decomposes in a concerted manner only and forms three HCN molecules (Ondrey and Bersohn 1984). These measurements provided an upper bound of the barrier to reaction (I) (115 kcal/mol). The results also indicate that the transition state for reaction (I) has three-fold symmetry. Evidence of a step-wise decomposition reaction,

$$\textit{sym}\text{-triazine} \rightarrow H_2C_2N_2 + \text{HCN} \rightarrow 3\ \text{HCN}, \tag{II}$$

was not observed. In the 248-nm experiments, the energy measured in the product translational and internal modes is consistent with an equipartitioning of the available product energy. The 193-nm experiments, however, showed a nonstatistical product energy distribution with 99% of the available product energy partitioned into the internal modes of the HCN products (Ondrey and Bersohn 1984). A time-resolved infrared fluorescence study of the HCN formed from 193-nm photolysis of *sym*-triazine showed that the HCN bending vibrations are excited preferentially, with "no evidence of a hot rotational population" (Goates, Chu, and Flynn 1984). A simple harmonic oscillator analysis of the products indicates that the bending quanta of HCN formed from photolysis of *sym*-triazine at 193 nm is 70 times larger than the number of C-H stretching quanta (Goates, Chu, and Flynn 1984).

The anomalous difference in the product energy distributions for the 248- and 193-nm photodissociation experiments was attributed to transitions to different excited states that subsequently

cross to the ground state potential energy surface at different regions of configuration space (Migrdichian 1947). The geometric structures, levels, and types of vibrational excitation in the ground-state molecule are dependent on the region of configuration space at which the crossings occur. If the transition results in a vibrationally excited and highly distorted ground-state molecule that reacts before vibrational or structural relaxation occurs, a nonstatistical partitioning of energy could result in the product molecules. This could explain the differences in product energy distributions for the two photolysis energies (Ondrey and Bersohn 1984).

The experiments clearly show that decomposition occurs in a concerted manner under 193- and 248-nm photolysis (Ondrey and Bersohn 1984; Goates, Chu, and Flynn 1984). Concerted triple dissociation reactions are uncommon, but not unknown. There are at least two other cyclic molecular systems that have also been shown to decompose through a concerted triple dissociation mechanism, *s*-tetrazine (King *et al.* 1977; Zhao *et al.* 1989) and 2,4,6-hexahydro-1,3,5-trinitro-1,3,5-triazine (Zhao, Hintsa, and Lee 1988).

Concerted triple association of three HCN molecules to form *sym*-triazine seems more improbable than the reverse reaction, the concerted triple dissociation in reaction (I). In a triple association reaction, entropic effects associated with bringing three HCN molecules together in a concerted fashion, especially in the gas phase, would seem so large as to prohibit reaction. However, entropic hindrance to association would be reduced if a prereaction intermediate with a structure favorable to concerted triple association could be easily formed. Experiment shows that such a species exists (Jucks and Miller 1988). It is a cyclic hydrogen-bonded cluster $(HCN)_3$. Rotationally resolved spectra of the infrared active doubly degenerate C-H stretch for the trimer cluster is consistent with an oblate planar symmetric top (Jucks and Miller 1988). Unfortunately, the experimental results could not provide details of this cyclic structure. Subsequent *ab initio* calculations on hydrogen-bonded $(HCN)_3$ clusters confirmed that the cyclic cluster exists in conjunction with linear HCN trimer chains (Kurnig, Lischka, and Karpfen 1990). Zero-point corrected relative energies of the two clusters differ by only 0.5 kcal/mol (Kurnig, Lischka, and Karpfen 1990). It is conceivable that HCN gas, under containment, would form clusters, including the hydrogen-bonded cyclic trimer. The HCN molecules, weakly bound in such a cyclic cluster, would then be in a sterically favorable arrangement for a concerted association:

$$3\ HCN \rightarrow (HCN)_3 \rightarrow \textit{sym}\text{-triazine}. \qquad \text{(III)}$$

Reaction energy appropriately imparted to the cluster would allow reaction (III) to occur.

The focus of this study is to investigate reaction mechanisms and energetics for the decomposition and formation of *sym*-triazine [reactions (I)–(III)]. We also investigate vibrational coupling of *sym*-triazine and the $(HCN)_3$ cluster with the reaction coordinate for reactions (I) and (III). Our results also examine basis set dependence for the calculations, as well as effects of increased electron correlation.

2. METHODS

All calculations reported in this work were done using the Gaussian 94 set of programs (Frisch *et al.* 1995). Critical points on the *sym*-triazine potential energy surface corresponding to reactions (I)–(III) were determined through MP2 geometry optimizations and characterized through normal mode analyses using the 6-31G** (Hehre, Ditchfield, and Pople 1972; Hariharan and Pople 1973; Gordon 1980), 6-311++G** (McLean and Chandler 1980; Krishnan et al. 1980), and cc-pVTZ (Woon and Dunning 1993; Kendall, Dunning, and Harrison 1972; Dunning 1989) basis sets. QCISD(T) energy refinements were calculated for each MP2-optimized structure with its corresponding basis set. All calculations were run with frozen core orbitals, and the geometry optimizations met the default convergence criteria given by Frisch *et al.* (1995). Intrinsic reaction coordinate (IRC) calculations were performed at the MP2/6-31G** level. The IRC calculation leading from the transition state structure of reaction (I) towards isolated HCN confirmed that this transition state is also the saddle point for reaction (III). All IRC calculations proceeded to minima as determined by the default convergence criteria in Frisch *et al.* (1995). Saddle points for reaction (II) were not determined for reasons discussed as follows.

3. RESULTS AND DISCUSSION

Molecular structures for *sym*-triazine, the dimer $H_2C_2N_2$, the cyclic $(HCN)_3$ cluster, the HCN molecule, and the transition state for reactions (I) and (III) are shown in Figure 1. Subsequent normal mode analyses characterized each species. The molecular properties are shown in Table 1. The atom labels in Table 1 are consistent with the structures shown in Figure 1, and the internal coordinates used in our discussion are shown in the transition state structure in Figure 1(b). Although the atoms are not labeled on the transition state structure in Figure 1(b), the labeling of the atoms follows the same pattern around the ring as in Figure 1(a). The internal coordinates shown in Figure 1(b) will be discussed next and are the same for all structures illustrated in Figure 1.

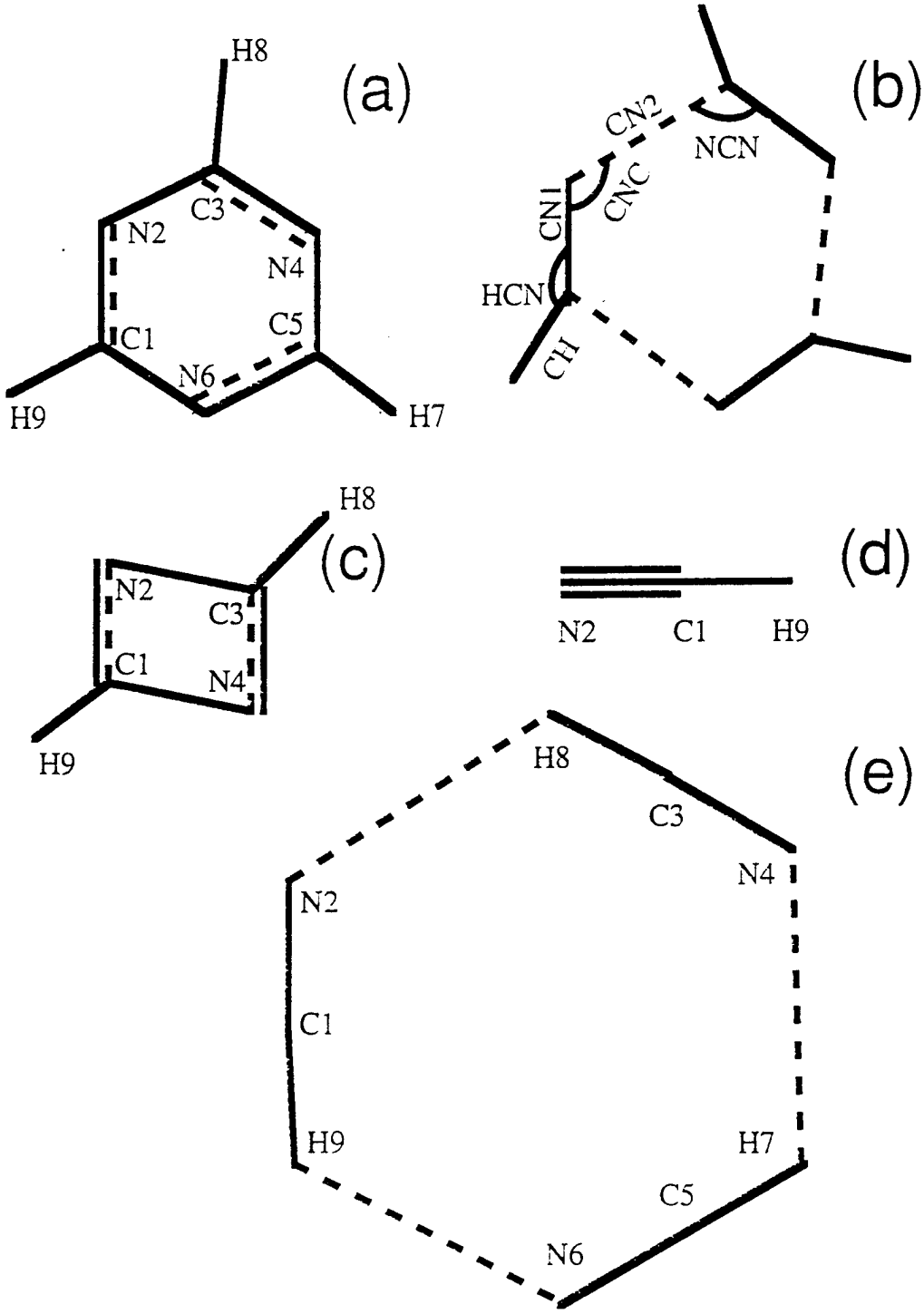

Figure 1. Structures of (a) *sym*-triazine; (b) transition state for the concerted triple dissociation and association reactions [reactions (I) and (III)]; (c) the stable dimer species H_2C_2N2 associated with the stepwise dissociation mechanism [reaction (II)]; (d) HCN; and (e) the hydrogen-bonded $(HCN)_3$ cluster located on the concerted triple association/dissociation path.

Table 1. MP2 Optimized Structural Parameters, Harmonic Frequencies, and Zero-Point Energies[a]

Parameter[f]	*sym*-triazine				TS(3HCN → *sym*-triazine)			HCN				$H_2C_2N_2$			$(HCN)_3$			
	6-31G**	6-311++G**	cc-pVTZ	Expt.[b,c]	6-31G**	6-311++G**	cc-pVTZ	6-31G**	6-311++G**	cc-pVTZ	Expt.[d]	6-31G**	6-311++G**	cc-pVTZ	6-31G**	6-311++G**	cc-pVTZ	ACPF[e]
Internal[f] Coordinates																		
C1N2	1.3404	1.3396	1.3351	1.338	1.2081	1.2039	1.1978	1.1778	1.1714	1.1668	1.1570	1.2893	1.2871	1.2837	1.1773	1.1710	1.1665	1.1595
C3N2	1.3404	1.3396	1.3351	1.338	1.9024	1.8941	1.8980					1.5369	1.5369	1.5339	3.1537	3.1682	3.1290	
C3N4	1.3404	1.3396	1.3351	1.338	1.2081	1.2039	1.1978					1.2895	1.2871	1.2837	1.1774	1.1710	1.1665	
C5N4	1.3404	1.3396	1.3351	1.338	1.9023	1.8941	1.8980								3.1539	3.1682	3.1291	
C5N6	1.3404	1.3396	1.3351	1.338	1.2081	1.2039	1.1978								1.1773	1.1710	1.1665	
C5H7	1.0833	1.0869	1.0822	1.084	1.0719	1.0756	1.0704	1.0649	1.0680	1.0643	1.0580		1.0893	1.0846	1.068	1.0707	1.0679	1.0711
C3H8	1.0833	1.0869	1.0822	1.084	1.0719	1.0756	1.0704					1.0845	1.0893	1.0846	1.068	1.0708	1.0679	
C1H9	1.0833	1.0869	1.0822	1.084	1.0719	1.0756	1.0704					1.0845	79.71	79.56	1.068	1.0707	1.0679	
C3N2C1	113.96	114.11	114.05	113.2	116.00	116.54	116.36					79.35	100.29	100.44				
N4C3N2	126.04	125.89	125.95	126.8	124.00	123.46	123.64					100.61						
C5N4C3	113.96	114.11	114.05	113.2	116.00	116.53	116.36											
N6C5N4	126.04	125.89	125.95	126.8	124.00	123.46	123.64											
N6C5H7	116.98	117.06	117.02	116.6	139.00	139.51	140.10	180.0	180.0	180.0	180.0				177.01	177.68	177.07	177.84
N4C3H8	116.98	117.06	117.02	116.6	139.00	139.51	140.10								177.01	177.68	177.06	
N2C1H9	116.98	117.06	117.02	116.6	139.00	139.50	140.10					131.91	132.30	131.84	177.01	177.68	177.07	
N2H8C3												131.88	132.30	131.84	122.13	119.45	121.48	118.0
H8N2C1															120.92	122.92	121.55	
N2H8															2.4532	2.5014	2.4359	2.5532
Harmonic Freq.																		
1	358	341	358	340	725*i*	725*i*	699*i*	725	730	719	712	438	419	428	50	46	53	52
2	358	341	358	340	151	120	140	725	730	719	712	737	734	725	50	46	53	52
3	687	686	683	675	151	120	141	2039	2016	2027	2089	791	790	806	83	74	82	83
4	687	686	683	675	307	309	316	3533	3483	3476	3312	882	881	880	83	74	82	83
5	770	744	772	737	307	309	316					919	886	934	105	102	109	103
6	921	895	940	925	361	332	353					1015	1006	993	136	121	134	135
7	1015	957	1009	992	551	552	551					1241	1211	1214	149	133	142	140
8	1027	957	1043	1031	551	552	551					1266	1239	1239	155	140	145	131
9	1027	1014	1043	1031	614	614	597					1625	1597	1596	155	140	145	131
10	1149	1140	1144	1132	784	770	786					1697	1672	1660	729	735	729	723
11	1212	1200	1199	1174	825	789	827					3258	3203	3204	730	735	729	723
12	1212	1200	1199	1174	825	789	827					3260	3205	3206	740	740	733	735
13	1256	1232	1243	1251	1011	1002	982								778	771	769	757
14	1430	1411	1405	1617	1095	1079	1058								778	771	769	757
15	1469	1452	1449	1410	1095	1080	1058								786	777	775	763
16	1469	1452	1449	1410	1789	1756	1780								2046	2023	2033	2166
17	1622	1600	1600	1556	1943	1915	1931								2046	2023	2033	2166
18	1622	1600	1600	1556	1943	1915	1931								2049	2025	2035	2172
19	3268	3221	3221	3056	3415	3357	3365								3496	3451	3433	3469
20	3268	3221	3221	3056	3415	3357	3365								3501[c]	3454[c]	3438[g]	3471
21	3272	3225	3225	3042	3418	3359	3367								3501[c]	3455[c]	3438[g]	3471
z.p.e	41.6	40.9	41.2	40.5	35.1	34.4	34.7	10.0	10.0	9.9	9.8	24.5	24.1	24.1	31.7	31.2	31.2	31.7

[a] Energies in kcal/mol, distances in Å, bond angles in degrees, and frequencies in cm^{-1}. [b] Lancaster and Stoicheff 1956. [c] Lancaster, Stamm, and Colthup 1961. [d] Herzberg 1945; Huber and Herzberg 1979. [e] Kurnig, Lischka, and Karpfen 1990. [f] Atom numbering illustrated in Figure 1. [g] Experimental value is 3273.545 cm^{-1} (Jucks and Miller 1988).

3.1 Geometries. All calculated structural parameters of *sym*-triazine are within 1% of the experimental values, showing very little variation with the size of the basis set. The HCN geometries are in good agreement with experiment for all the basis sets, with the errors ranging from <2% (6-31G**) to <1% (cc-pVTZ). The structure of the $(HCN)_3$ cluster has not been determined experimentally, although Jucks and Miller (1988) suggest two structures that are consistent with the rotational constants determined from the rovibrational spectrum of the C-H asymmetric stretch. The intermolecular C-C distances for the two structures suggested by Jucks and Miller are 3.62 and 3.83 Å, respectively. The C-C internuclear distances of the $(HCN)_3$ clusters calculated using the 6-31G**, 6-311++G**, and cc-pVTZ basis sets are 3.63, 3.66, and 3.60 Å, respectively. These distances are consistent with those of Structure A in Figure 5 of Jucks and Miller (1988). *Ab initio* calculations using the average coupled pair approximation (ACPF) method and extended basis sets (Kurnig, Lischka, and Karpfen 1990) predicted the cyclic trimer with N-H intermolecular distances of 2.5532 Å. Comparison of our results with the ACPF calculations is shown in Table 1. The structures from the two methods are similar. The cyclic cluster, illustrated in Figure 1(e), consists of three linear HCN molecules with H-N distances of 2.5 Å.

Structures and energies along the reaction coordinate determined from MP2/6-31G** IRC calculations are shown in Figure 2. The structures along the reaction path have three-fold symmetry. Because of this, there are six unique internal coordinates that describe the geometric changes along the reaction path and are defined in Figure 1(b). These unique internal coordinates include two types of C-N bonds: one that becomes intermolecular in the $(HCN)_3$ cluster (denoted CN2), and one that remains an intramolecular bond along the reaction path (denoted CN1). The C-H distances and HCN, NCN, and CNC angles make up the rest of the six internal coordinates. Changes of these internal coordinates along the reaction path are shown in Figure 3. Negative values of the reaction coordinate correspond to the $(HCN)_3$ cluster region of the PES, and positive values along the reaction coordinate correspond to the *sym*-triazine region of the PES. The reaction path coordinate value 0.0 corresponds to the transition state connecting the $(HCN)_3$ cluster and *sym*-triazine minima. The internal coordinates that change the most along this reaction path are the CN2 bond length and the HCN angle. The CN2 bond increases almost linearly as the *sym*-triazine dissociation progresses to the $(HCN)_3$ cluster. The other CN bond type, CN1, becomes shorter as *sym*-triazine decomposes, and almost equals the equilibrium CN bond distance in the $(HCN)_3$ cluster and isolated HCN by the time it reaches the saddle point. The CN1 bond distance changes only slightly as the $(HCN)_3$ minimum is approached after crossing the saddle point. The C-H bond distances do not change significantly during the reaction. The HCN angle increases almost monotonically as the $(HCN)_3$

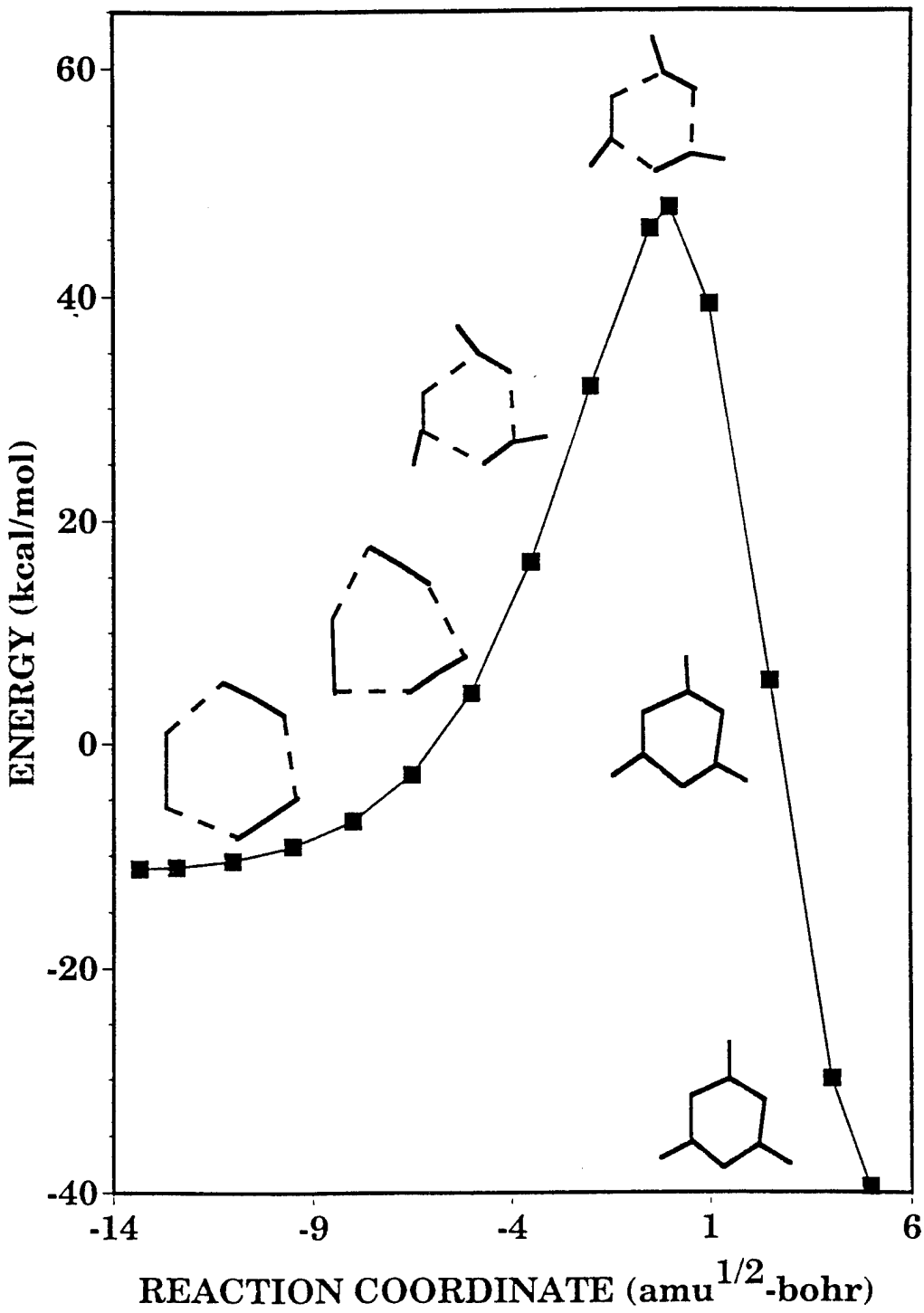

Figure 2. MP2/6-31G** reaction path from the IRC calculation for reactions (I) and (III). Every tenth point of the IRC is shown. In addition to the stable and transition state structures, three other structures along the reaction path have been shown to enable the reader to visualize the mechanism of concerted triple association and dissociation. The $(HCN)_3$ is illustrated in the far-left structure of the figure. The *sym*-triazine molecule is represented by the far-right structure of the figure.

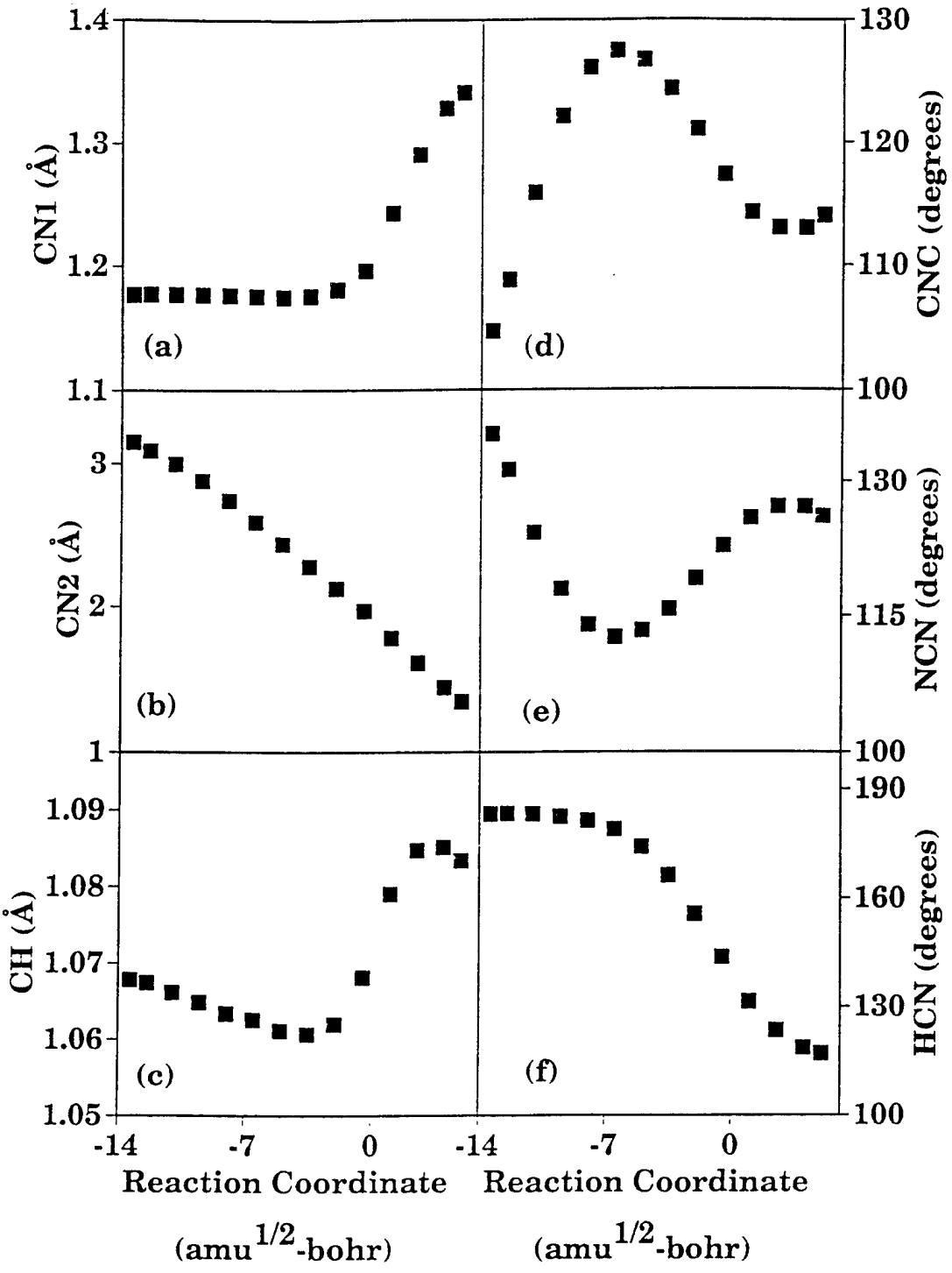

Figure 3. Internal coordinate changes along the MP2/6-31G** IRC for the concerted triple association/ dissociation reactions. For definition of internal coordinates, see Figure 1(c).

cluster is approached. This angle varies from 117° in *sym*-triazine to 139° at the transition state. It continues to open up to 180° in the $(HCN)_3$ cluster region. The ring angles, NCN and CNC, do not show monotonic behavior. The NCN angle first decreases after crossing the transition state and then opens up rapidly as the molecule approaches the cluster minimum. The changes in the CNC angle along the reaction path behave in an almost equal but opposite manner to the changes in the NCN angles.

Attempts were made to locate transition states leading to dimer formation and decomposition and stable structures starting from various dimer configurations. The only structure located corresponds to a local minimum on the PES. Its structure is that of a parallelogram of the heavy atoms with internal angles for CNC and NCN of 100° and 79°, respectively [Figure 1(c)]. The HCN angles are far from linear in this structure (see Table 1).

3.2 Frequencies. MP2 harmonic vibrational frequencies of the critical points described previously were calculated using the aforementioned basis sets and are shown in Table 1. MP2/cc-pVTZ eigenvectors and corresponding harmonic frequencies of all critical points (except HCN) for reactions (I) and (III) are shown in Figures 4–6. The predicted frequencies of HCN agree with experiment to within 7% for all basis sets. Predictions of *sym*-triazine frequencies are within 7.5% of experimental values for all basis sets. There is only one vibration that has been measured and assigned for the $(HCN)_3$ cluster. It corresponds to the doubly degenerate C-H asymmetric stretch at 3274 cm^{-1} and contains rotationally resolved bands (Jucks and Miller 1988). Our value at 3438 cm^{-1} is 5% higher than the experimental value. Jucks and Miller provide rotational constants $A''=B''=2C''=0.0822$ cm^{-1} determined from fits to the rotational transitions for a planar oblate symmetric top (Jucks and Miller 1988). Our calculated values using the 6-31G**, 6-311++G**, and cc-pVTZ basis sets are 0.0827, 0.0821, and 0.0840 cm^{-1}, respectively.

Lancaster, Stamm, and Colthup (1961) reported the infrared and Raman spectra for *sym*-triazine and made band assignments based upon a normal coordinate analysis. Using the description of the modes given by Lancaster, Stamm, and Colthup, we were able to match all vibrational modes to experimental assignments except for the experimental modes ν_4 (1617 cm^{-1}), ν_8 (1410 cm^{-1}), and ν_9 (1174 cm^{-1}). Lancaster, Stamm, and Colthup predicted doubly degenerate modes ν_8 and ν_9 should correspond to ring and C-H rocking vibrations, respectively. If we assume that the MP2/cc-pVTZ modes with frequency 1449 cm^{-1} can be assigned to experimental ν_8 and the modes with frequency 1199 cm^{-1} to experimental

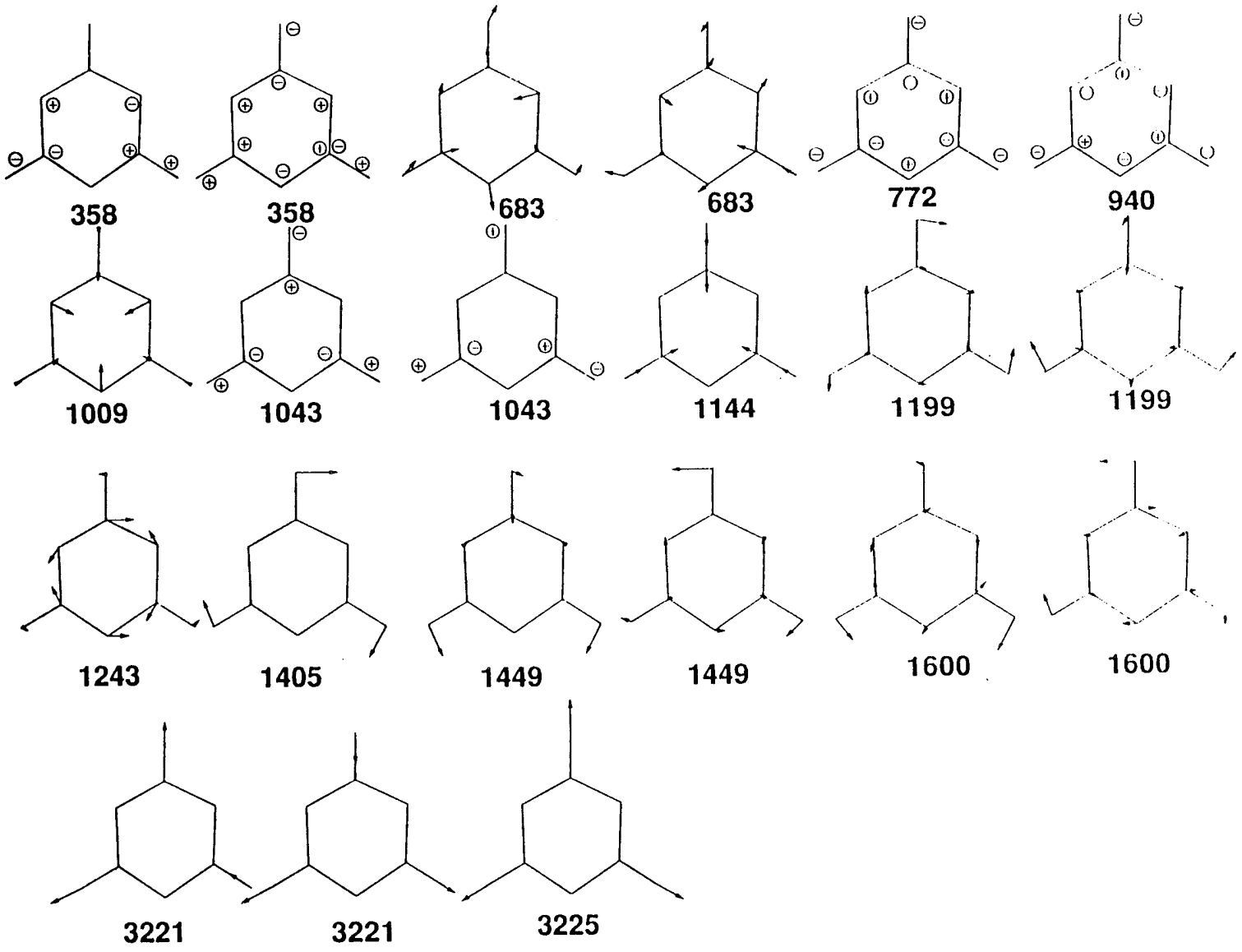

Figure 4. MP2/cc-pVTZ vibrational eigenvectors for *sym*-triazine. Positive and negative signs denote out-of-plane motion. Each eigenvector is labeled with its corresponding frequency (in cm^{-1}).

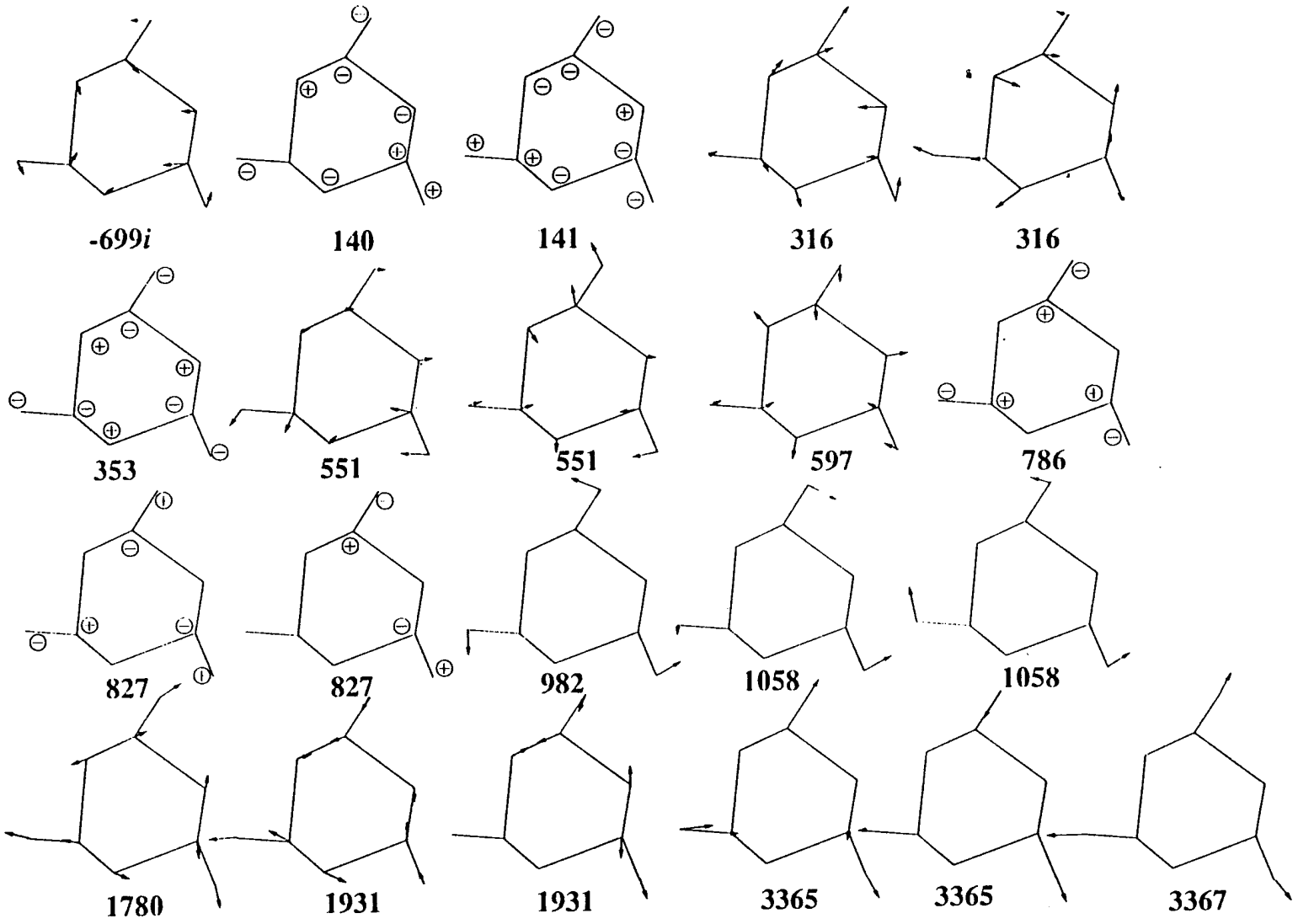

Figure 5. MP2/cc-pVTZ vibrational eigenvectors for the transition state leading to concerted triple dissociation/association of *sym*-triazine [reactions (I) and (III)]. Positive and negative signs denote out-of-plane motion. Each eigenvector is labeled with its corresponding frequency (in cm^{-1}).

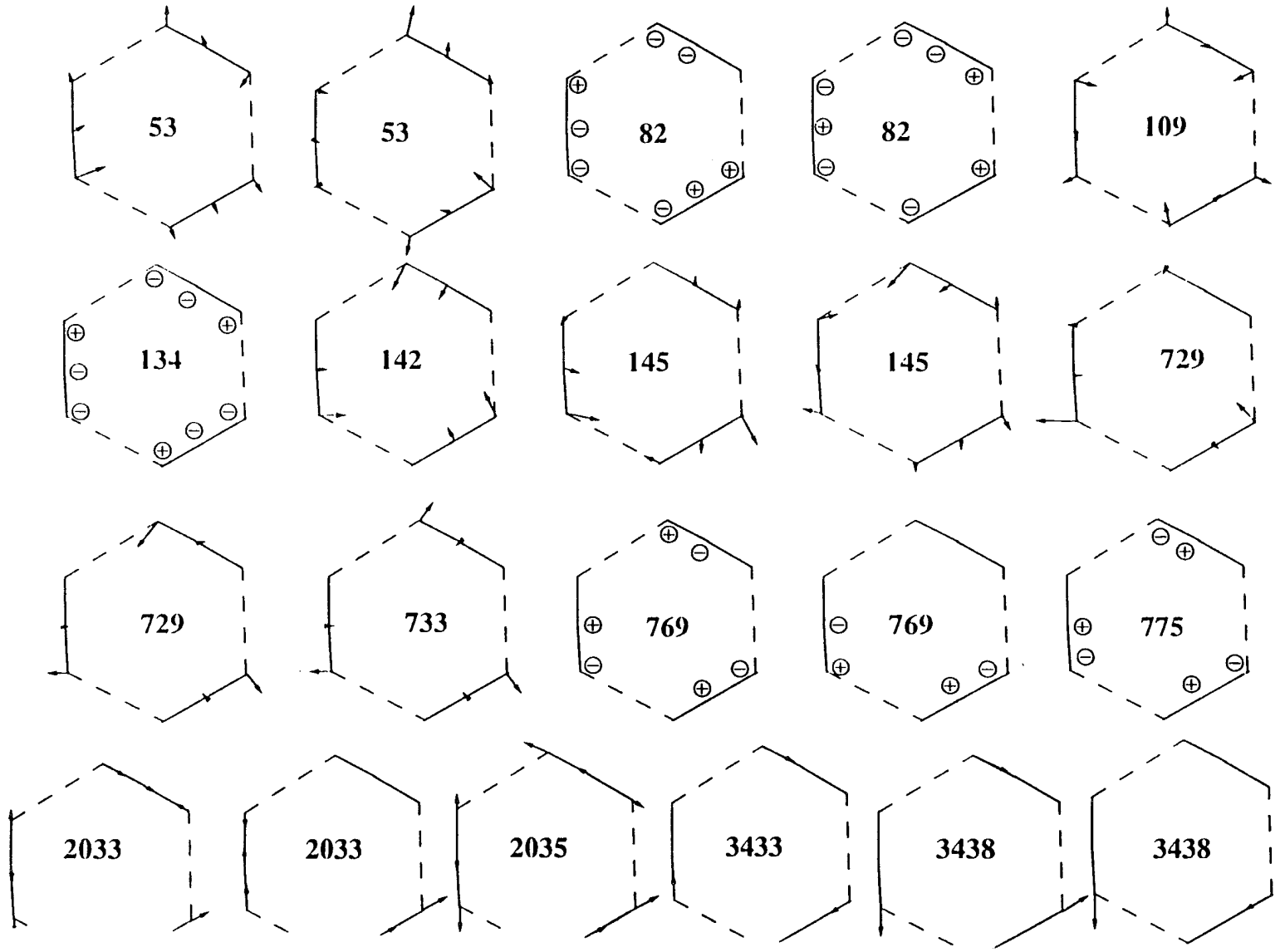

Figure 6. MP2/cc-pVTZ vibrational eigenvectors for the $(HCN)_3$ cluster. Positive and negative signs denote out-of-plane motion. Each eigenvector is labeled with its corresponding frequency (in cm^{-1}).

ν_9, then the *ab initio* predictions agree with experiment to within 3%. Visual inspection of the MP2/cc-pVTZ eigenvectors corresponding to *ab initio* frequencies 1449 and 1199 cm^{-1} indicate that these two sets of degenerate vibrations cannot be distinctly classified as C-H rocks or ring vibrations. The remaining *ab initio* eigenvector that we could not assign to anything else (1405 cm^{-1}) was assigned to experimental mode ν_4 with 13% disagreement. However, mode ν_4 is one of the two A'_2 fundamentals that are inactive and were not observed (Jucks and Miller 1988). The frequency for this fundamental that was reported by Lancaster, Stamm, and Colthup (1961) was calculated from estimated force constants and considered "very approximate."

The zero-point energies for *sym*-triazine with the 6-31G**, 6-311++G**, and the cc-pVTZ basis sets are 41.6, 40.9, and 41.2 kcal/mol, respectively, and compare well with experimental zero-point energy of 40.5 kcal/mol (Lancaster, Stamm, and Colthup 1961). The HCN zero-point energies for the three basis sets (ranging from 9.9 to 10.0 kcal/mol) agree well with the experimental value (9.8 kcal/mol) (Herzberg 1945; Huber and Herzberg 1979).

3.3 Vibrational Coupling. It has been shown that projection of the eigenvector of a vibrational mode onto the eigenvector corresponding to the direction along the reaction path is related to the coupling of that vibrational mode with the reaction coordinate (Waite and Miller 1981; Rice, Grosh, and Thompson 1995). Waite and Miller showed that the unimolecular decay rates of the Henon-Heiles model behave statistically for all energies, even though this system has quasiperiodic classical motion at low energies, conditions under which mode specificity might be expected (Waite and Miller 1981). They suggested that the statistical behavior was due to coupling of the intramolecular motions of the model with the dissociative reaction coordinates for the system, since there was some degree of projection of all of the vibrational modes onto the reaction coordinates for the Henon-Heiles model. In other words, there were no vibrational modes in which energy could be trapped. To further investigate the role of vibrational coupling with the reaction coordinate, they modified the Henon-Heiles potential such that vibrational modes exist that do not project onto the reaction coordinate (Waite and Miller 1981). Mode specificity in the decomposition was then induced. Rice, Grosh, and Thompson (1995) showed that rates of unimolecular decomposition through competing channels were enhanced and branching ratios changed upon excitation of vibrational modes of a reactant that project strongly onto the reaction coordinates of the system (Rice, Grosh, and Thompson 1995). Our goal in this section is not to investigate mode-specific dynamics for this system. Rather we wish to determine which of the intramolecular motions of *sym*-triazine and the $(HCN)_3$ cluster couple most strongly with the reaction coordinate for reactions (I) and (III). This will suggest mechanisms for energy transfer from excited vibrational modes to the reaction

coordinate. The studies by Waite and Miller (1981) and Rice, Grosh, and Thompson (1995) have clearly shown a correlation between projection of vibrational modes onto the reaction coordinate and coupling with the reaction coordinate. Thus, similar analyses based on projections of the vibrational modes of *sym*-triazine and the $(HCN)_3$ cluster onto the reaction coordinate should verify whether the intramolecular motions of these molecules are coupled with the reaction path.

As set forth in Rice, Grosh, and Thompson (1995), we calculated local normal modes (Miller, Handy, and Adams 1980) for points along the reaction path for reaction (III) at the MP2/6-31G** level. The infinitesimal translations and rotations were projected out, leaving 3N-7 vibrational modes of the molecule and the eigenvector corresponding to the direction along the reaction path (Miller, Handy, and Adams 1980). We projected the eigenvectors corresponding to the harmonic vibrational frequencies of equilibrium *sym*-triazine and the $(HCN)_3$ cluster onto the eigenvector associated with the direction along the reaction path (Miller, Handy, and Adams 1980) for selected reaction coordinate values. The results of the projections of *sym*-triazine and the $(HCN)_3$ cluster vibrational eigenvectors onto the reaction path eigenvectors are shown in Figures 7 and 8, respectively. Only those modes that have projections greater than 0.05 are shown in these figures. There are three vibrational modes of *sym*-triazine that project strongly all along the reaction path for reactions (I) and (III); they correspond to 1015, 1149, and 1430 cm^{-1}. These modes correspond to two ring symmetric breathing modes and an HCN symmetric bending mode, respectively. Additionally, a fourth vibrational mode (1256 cm^{-1}) projects onto portions of the reaction path, but its projection is not as strong as the other vibrational modes. Its motion can best be described as being the most similar to the eigenvector associated with the imaginary frequency at the saddle point (see Figure 5). There are two vibrational modes for the $(HCN)_3$ cluster that project strongly onto the reaction path; these are both symmetric ring-breathing modes (105 and 149 cm^{-1}). Two other modes project less strongly onto the reaction path (740 and 3496 cm^{-1}); both consist mainly of hydrogenic motions.

It is clear that there are intramolecular motions of *sym*-triazine and the $(HCN)_3$ cluster that couple strongly with the reaction coordinate, indicating the most likely routes through which reaction energy distributed in either of these species can transfer efficiently to the reaction coordinate for reactions (I) and (III).

3.4 Energetics. The relative and absolute energies of each critical point calculated at the MP2 and QCISD(T) levels with the three different basis sets for *sym*-triazine, $H_2C_2N_2$, the $(HCN)_3$ cluster, HCN,

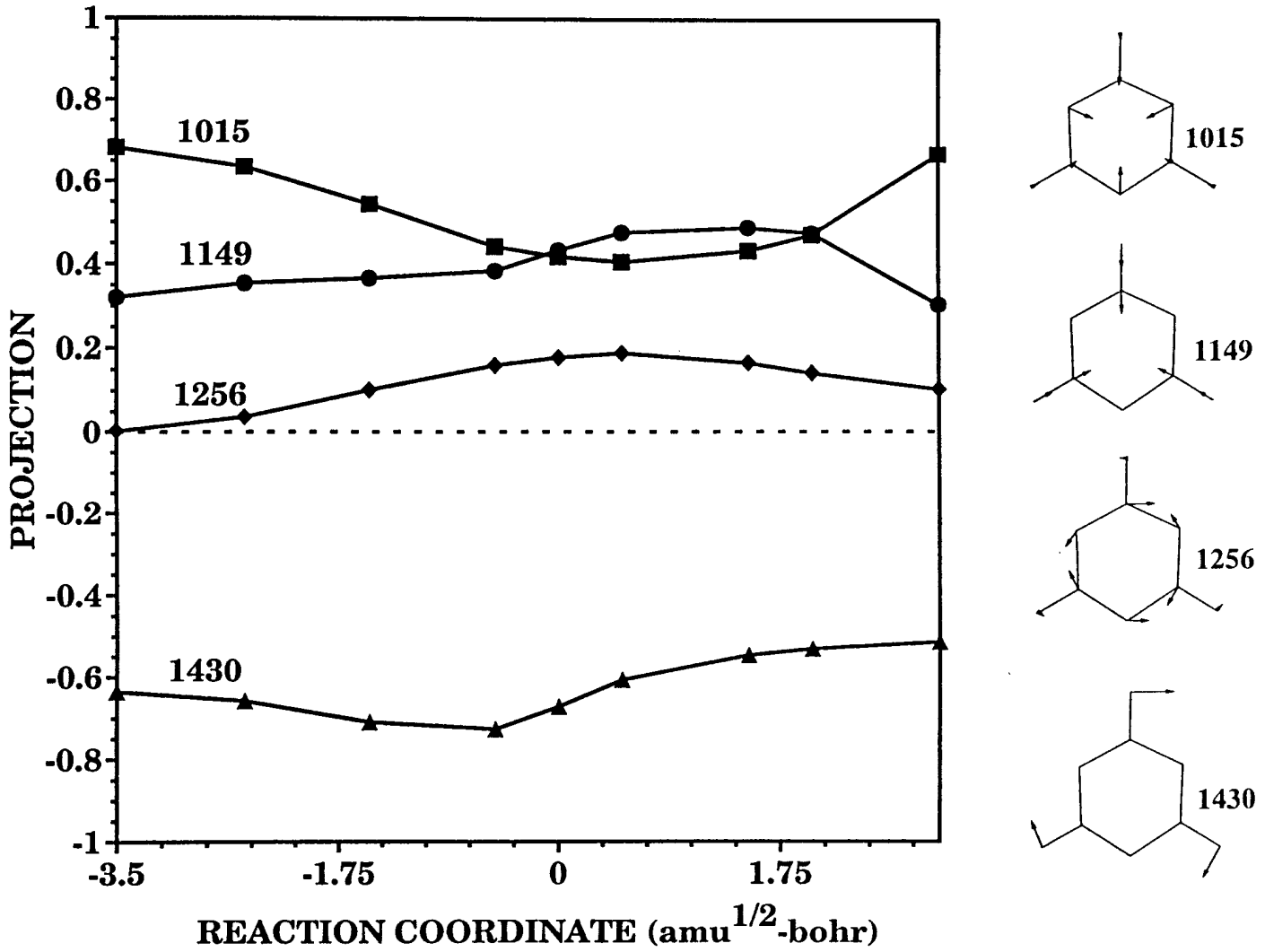

Figure 7. Projection of the eigenvectors corresponding to the MP2/6-31G** harmonic vibrational frequencies of *sym*-triazine onto eigenvectors for points on the reaction path that correspond to the direction along the path for the concerted triple association/decomposition reactions [reactions (I) and (III)]. Eigenvectors with projections greater than 0.05 are illustrated, and labeled with the corresponding MP2/6-31G** harmonic vibrational frequency (in cm^{-1}).

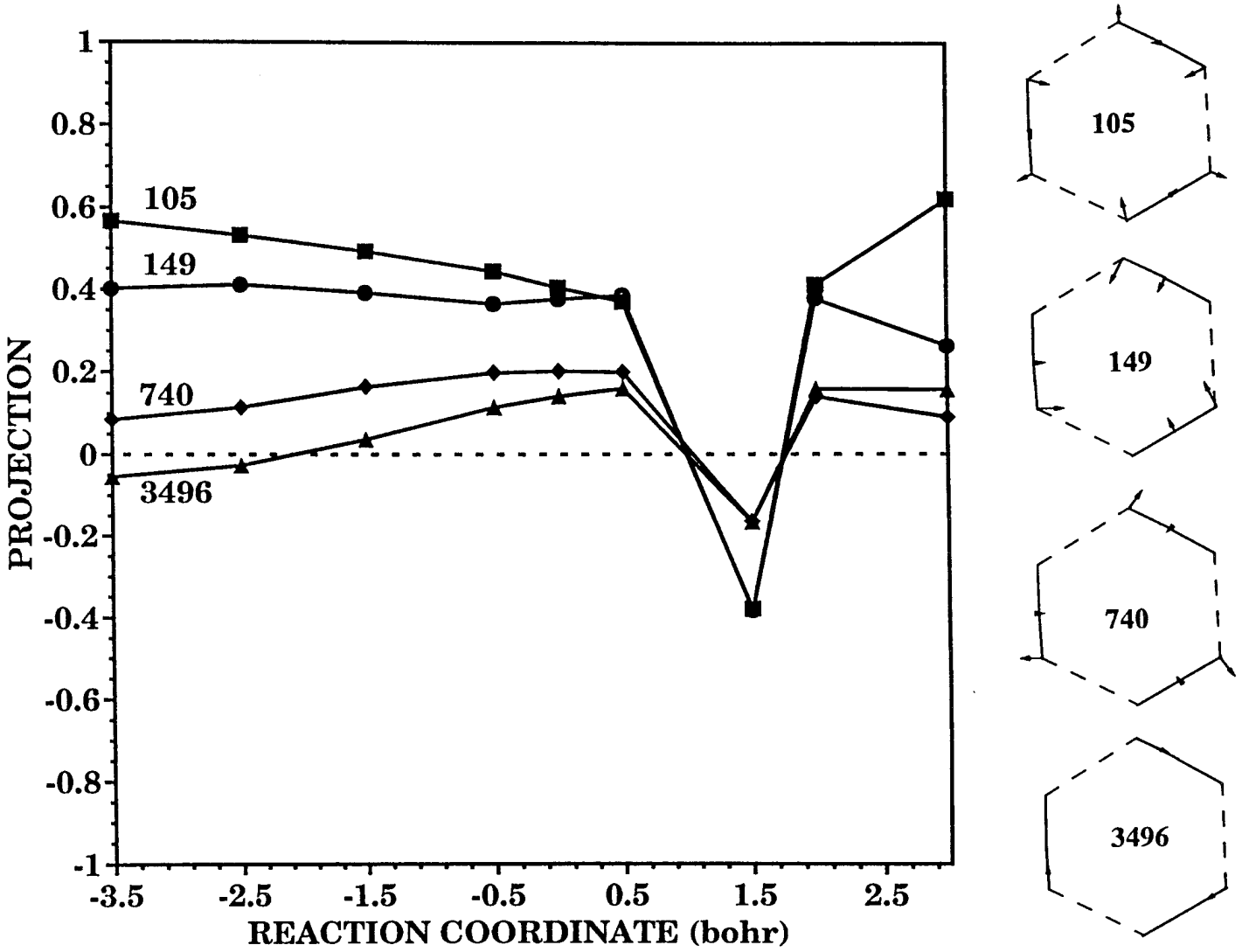

Figure 8. Projection of the eigenvectors corresponding to the MP2/6-31G** harmonic vibrational frequencies of the $(HCN)_3$ cluster onto eigenvectors for points on the reaction path that correspond to the direction along the path for the concerted triple association/ decomposition reactions [reactions (I) and (III)]. Eigenvectors with projections greater than 0.05 are illustrated, and labeled with the corresponding MP2/6-31G** harmonic vibrational frequency (in cm^{-1}).

and the saddlepoint are listed in Table 2. (A comparison of the zero-point-energy-corrected MP2 barriers to formation of *sym*-triazine from the $(HCN)_3$ cluster and to decomposition of *sym*-triazine with QCISD(T) for all the basis sets is shown in Figure 9.) The MP2/6-31G** and MP2/6-311++G** calculations predict similar barrier heights for the formation of *sym*-triazine from the $(HCN)_3$ cluster (62.2 and 62.4 kcal/mol, respectively). The MP2/cc-pVTZ prediction of this barrier is lower (57.4 kcal/mol). QCISD(T) energy refinements for the 6-31G** and 6-311++G** barriers decrease the MP2 results slightly (61.1 and 61.7 kcal/mol, respectively). The QCISD(T) refinement of the MP2/cc-pVTZ barrier, however, increases the MP2 result by 0.7 kcal/mol (58.1 kcal/mol). Thermal activation barriers for this reaction have not been determined experimentally; thus, we cannot gauge the accuracy of these barrier heights. The only information about the barrier height for the formation of *sym*-triazine from isolated HCN is an upper limit of 72 kcal/mol (Ondrey and Bersohn 1984). Our values are well under this limit.

The zero-point-corrected MP2 barriers to decomposition of *sym*-triazine for the 6-31G**, 6-311++G**, and cc-pVTZ basis sets are 80.7, 77.7, and 79.6 kcal/mol, respectively. QCISD(T) refinements of the barriers for these three basis sets are 81.6, 79.0, and 81.2 kcal/mol, respectively; well below the experimental upper limit of 115 kcal/mol (Ondrey and Bersohn 1984). QCISD(T) energy refinements did not significantly change the MP2 results. Both reactions, however, showed some sensitivity to basis set size.

Experimental and calculated reaction enthalpies (corrected to T=298 K) for reaction (I) are given in Table 3. The calculated reaction enthalpies for reaction (I) range from 27.8 to 35.5 kcal/mol, at least 18% lower than the experimental value of 43.2 kcal/mol (Ondrey and Bersohn 1984). The QCISD(T)//MP2/ cc-pVTZ value of 35.5 kcal/mol is in closest agreement with experiment. The formation enthalpies of the $(HCN)_3$ cluster and $H_2C_2N_2$ + HCN from 3 HCN are also shown in Table 3.

The zero-point-corrected MP2 energies of the $H_2C_2N_2$ [Figure 1(c)] plus HCN relative to isolated HCN are 63.8, 64.0, and 61.3 kcal/mol for the 6-31G**, 6311++G**, and cc-pVTZ basis sets, respectively. Corresponding zero-point-corrected QCISD(T) values are 57.4, 57.6, and 55.9 kcal/mol. These values are higher than the zero-point-energy-corrected barriers to concerted triple association at all levels for each basis set, with a difference of 6.7 kcal/mol at the highest level of theory. Figure 10 illustrates this for the QCISD(T)/cc-pVTZ results. Even if we assume that there are no barriers to

Table 2. Absolute Energies (Hartrees) and Relative Energies With and Without Zero-Point Energy (ZPE) Corrections (kcal/mol) of Species on the *sym*-Triazine Potential Energy Surface

Level of Theory	$H_2C_2N_2$ + HCN	3HCN	TS(*sym*-triazine → $(HCN)_3$)	*sym*-triazine	$(HCN)_3$
Absolute Energies					
MP2//MP2/6-31G**	−279.4040456	−279.4985190	−279.4225671	−279.5614678	−279.5162594
QCISD(T)//MP2/6-31G**	−279.4746539	−279.5589918	−279.4839155	−279.6242656	−279.5758546
MP2//MP2/6-311++G**	−279.5142545	−279.6096735	−279.5319344	−279.6661137	−279.6262566
QCISD(T)//MP2/6311++G**	−279.5865234	−279.6717324	−279.5945901	−279.7308072	−279.6877556
MP2//MP2/cc-pVTZ	−279.6699089	−279.7607679	−279.6923459	−279.8296494	−279.7782811
QCISD(T)//MP2/cc-pVTZ	−279.7449569	−279.8271414	−279.7566438	−279.8963920	−279.8436781
Relative Energies					
MP2//MP2/6-31G**	59.3	0.0	47.7	−39.5	−11.1
QCISD(T)//MP2/6-31G**	52.9	0.0	47.1	−41.0	−10.6
MP2//MP2/6-311++G**	59.9	0.0	48.8	−35.4	−10.4
QCISD(T)//MP2/6311++G**	53.5	0.0	48.4	−37.1	−10.1
MP2//MP2/cc-pVTZ	57.0	0.0	42.9	−43.2	−11.0
QCISD(T)//MP2/cc-pVTZ	51.6	0.0	44.2	−43.5	−10.4
ZPE-Corrected Relative Energies					
MP2//MP2/6-31G**	63.8	0.0	52.8	−27.9	−9.4
QCISD(T)//MP2/6-31G**	57.4	0.0	52.2	−29.4	−8.9
MP2//MP2/6-311++G**	64.0	0.0	53.2	−24.5	−9.2
QCISD(T)//MP2/6311++G**	57.6	0.0	52.8	−26.2	−8.9
MP2//MP2/cc-pVTZ	61.3	0.0	47.9	−31.7	−9.5
QCISD(T)//MP2/cc-pVTZ	55.9	0.0	49.2	−32.0	−8.9

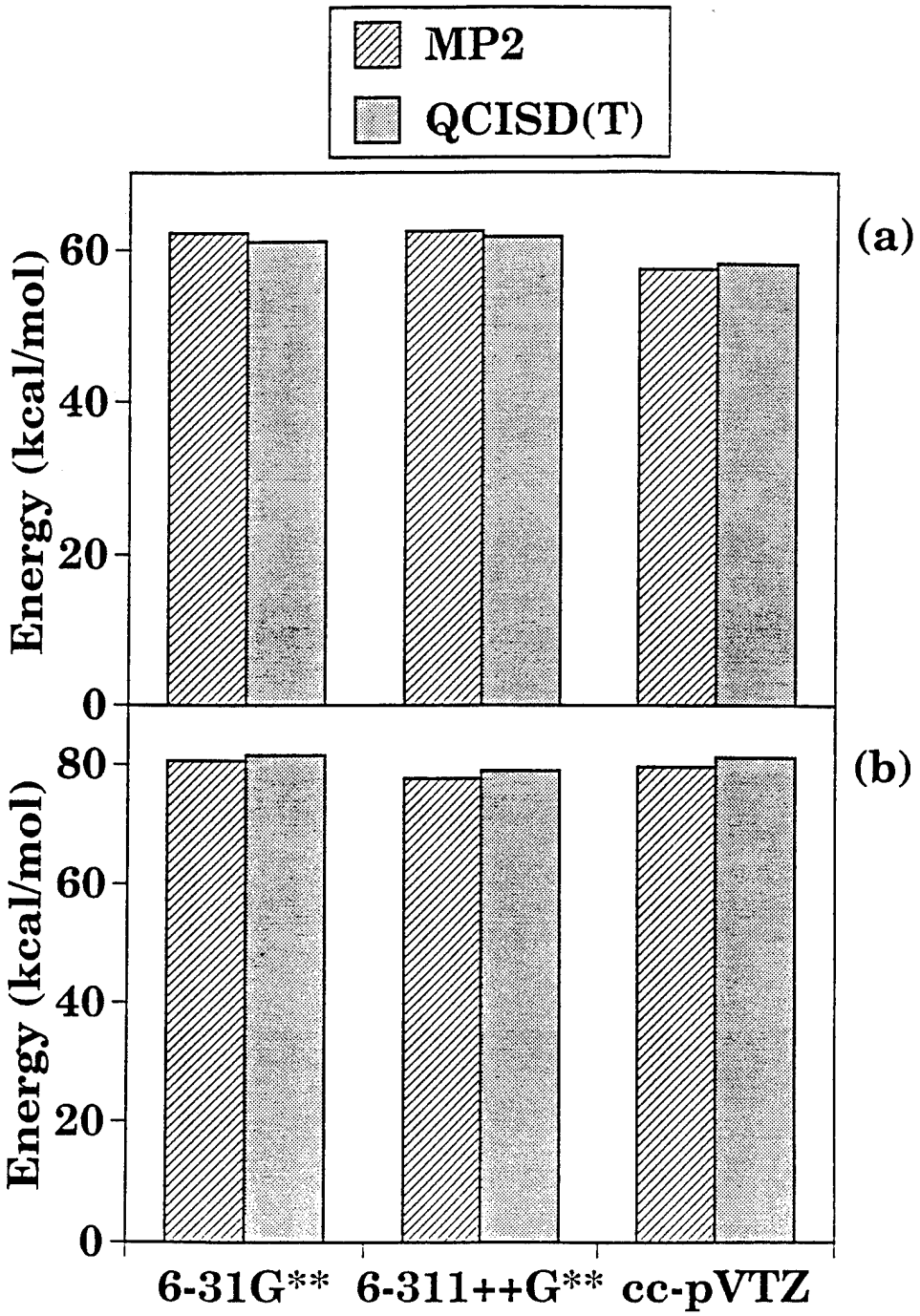

Figure 9. Comparison of MP2 and QCISD(T) (a) barriers to the formation of *sym*-triazine; and (b) barriers to decomposition of *sym*-triazine. The barriers are calculated for each of the given basis sets and are corrected for MP2 zero-point energies.

Table 3. Temperature-Corrected (T-298 K) Enthalpies (kcal/mol)

Level of Theory	Reaction Endothermicity
sym-triazine → 3HCN	
Experiment[a]	43.2
MP2//MP2/6-31G**	31.5
QCISD(T)//MP2/6-31G**	33.0
MP2//MP2/6-311++G**	27.8
QCISD(T)//MP2/6311++G**	29.5
MP2//MP2/cc-pVTZ	35.2
QCISD(T)//MP2/cc-pVTZ	35.5
$3HCN \rightarrow (HCN)_3$	
MP2//MP2/6-31G**	−9.4
QCISD(T)//MP2/6-31G**	−8.9
MP2//MP2/6-311++G**	−8.7
QCISD(T)//MP2/6311++G**	−8.4
MP2//MP2/cc-pVTZ	−9.3
QCISD(T)//MP2/cc-pVTZ	−8.7
$3HCN \rightarrow H_2C_2N_2 + HCN$	
MP2//MP2/6-31G**	62.1
QCISD(T)//MP2/6-31G**	55.7
MP2//MP2/6-311++G**	62.5
QCISD(T)//MP2/6311++G**	56.1
MP2//MP2/cc-pVTZ	59.7
QCISD(T)//MP2/cc-pVTZ	54.3

[a] Ondrey and Bersohn 1984.

formation of $H_2C_2N_2$ or the necessary HCN insertion into the $H_2C_2N_2$ molecule to form *sym*-triazine [reverse of reaction (II)], comparing the relative energies of the $H_2C_2N_2$ + HCN minimum and the saddle point for reaction (III) indicates that the reaction (II) pathway is higher in energy than that of the concerted triple association reaction (III). Because we are interested mainly in the low-energy pathway for the formation/decomposition reactions of *sym*-triazine, we did not investigate this reaction path further. We attempted to locate additional dimer structures, but none were found.

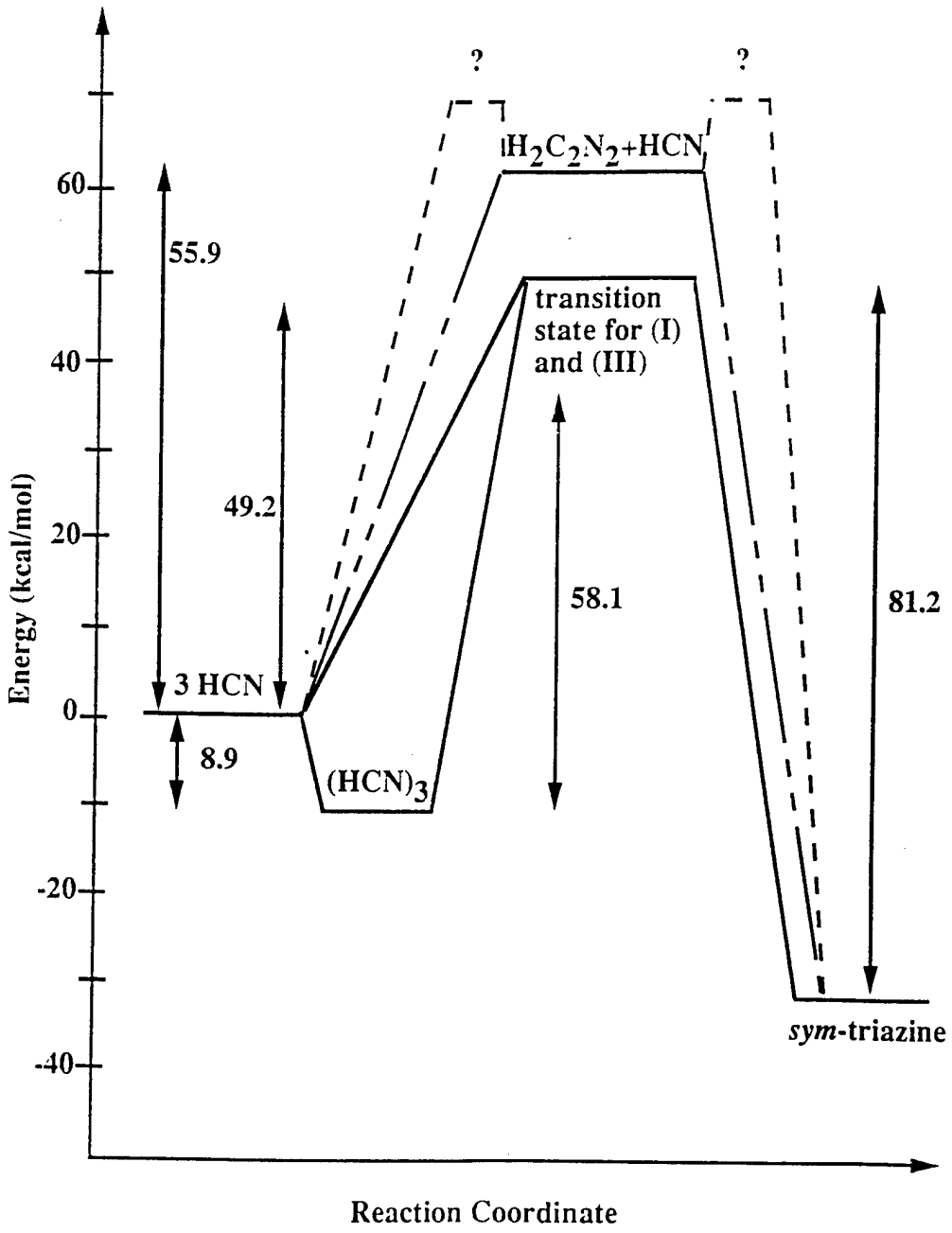

Figure 10. Schematic of the overall energetics for the reactions 3HCN → *sym*-triazine. Zero-point-corrected energies at the QCISD(T)//MP2/cc-pVTZ level are listed in kcal/mole. The higher energy pathway is the stepwise association mechanism [reverse of reaction (II)]; the lower energy path is the concerted triple association mechanism [reaction (I)].

These results support the experimental observations for reaction (I) (Ondrey and Bersohn 1984; Goates, Chu, and Flynn 1984). First, the zero-point-energy-corrected barrier for *sym*-triazine decomposition [reaction (I)] is within the experimentally determined upper limit. Secondly, the low-energy decomposition reaction is a concerted triple dissociation rather than a step-wise decomposition reaction such as reaction (II), in agreement with the photodissociation experimental results. Additionally, the structures of species along the reaction path for this process could explain the observed nonstatistical energy distribution in the bending mode over the stretches (Goates, Chu, and Flynn 1984). The saddle point structure for this reaction is similar to that of *sym*-triazine. The HCN angles in this structure are 140°. Thus, once this barrier is overcome and the system is in the HCN region of the potential energy surface, the HCN angles must open up 40° to reach both the $(HCN)_3$ cluster and HCN product values of 180°. The large change in the HCN angle of the transition state species to the cluster/isolated HCN molecules could be the source of the large HCN bending excitation that was observed by Goates, Chu, and Flynn (1984) in their study of the product energy distributions of *sym*-triazine photodissociation at 193 nm. The CN and CH bond distances, on the other hand, differ at most by 5% between the saddle point and cyclic $(HCN)_3$ cluster geometries. Thus, the most significant geometric changes in these internal coordinates have occurred before the saddle point is reached and could explain why vibrations corresponding to CN and CH stretches were not excited upon decomposition.

Our reaction path calculations indicate that the weakly bound cyclic $(HCN)_3$ cluster is a reaction intermediate on the *sym*-triazine decomposition pathway. However, the energy available to products upon crossing the reaction barrier is so large that this reaction intermediate would not be long-lived and probably not detectable during the decomposition process. Our results clearly show that the low-energy path to dissociation of *sym*-triazine is through a concerted triple dissociation. We were unable to locate a saddle point for decomposition of the $(HCN)_3$ cluster to form isolated HCN. Thus, we are assuming that the barrier to $(HCN)_3$ decomposition toward isolated HCN is merely the endothermicity of the cluster relative to isolated HCN.

4. CONCLUSIONS

We have presented an *ab initio* study of formation and decomposition reactions of *sym*-triazine. Two decomposition pathways were examined: a concerted triple decomposition reaction

$$\textit{sym}\text{-triazine} \rightarrow 3\ HCN \qquad (I)$$

and a stepwise decomposition reaction

$$sym\text{-triazine} \rightarrow H_2C_2N_2 + HCN \rightarrow 3\ HCN. \qquad (II)$$

Our best estimate of the energy required for reactions (I) and (II) are 81.2 and 87.0 kcal/mol [QCISD(T)// MP2/cc-pVTZ], respectively. These predicted energy requirements for reactions (I) and (II) are well below the experimentally determined upper bound (115 kcal/mol)[2].

IRC calculations starting from the transition state of reaction (I) toward isolated HCN led to a local minimum on the potential energy surface that corresponds to a weakly bound cyclic $(HCN)_3$ cluster. Thus, the reaction path connects the *sym*-triazine minimum with the cyclic $(HCN)_3$ cluster, a reaction intermediate leading to isolated HCN. Our best estimate of its energy relative to isolated HCN is −8.9 kcal/mol [QCISD(T)//MP2/cc-pVTZ]. The reverse of reaction (I), the association of HCN molecules to form *sym*-triazine, is therefore

$$3\ HCN \rightarrow (HCN)_3 \rightarrow sym\text{-triazine}. \qquad (III)$$

It is likely that formation of the $(HCN)_3$ cluster is a critical step in the association reaction (III) as it removes significant steric hindrance to the concerted triple association of the HCN molecules to form *sym*-triazine. However, this cluster is probably very short lived upon decomposition of *sym*-triazine, due to the excess energy available to products upon crossing the saddle point for reaction (I).

The zero-point-energy-corrected reaction barrier to triple association [reaction (III)] is lower than the energy needed to form the HCN + $H_2C_2N_2$, the stable intermediate complex for the step-wise reaction for formation or decomposition of *sym*-triazine for all basis sets and all levels of electron correlation. Our best estimate of the energy difference between HCN + $H_2C_2N_2$ and the barrier to triple association (relative to isolated HCN) is 6.7 kcal/mol [QCISD(T)//MP2/cc-pVTZ]. Any energy barrier to formation of $H_2C_2N_2$ or insertion of a third HCN into this intermediate to form *sym*-triazine cannot be lower than the energy of this intermediate. Thus, a step-wise reaction for formation or decomposition of *sym*-triazine is eliminated as the low-energy path in favor of the concerted route.

Critical points on the *sym*-triazine potential energy surface were located through MP2 geometry optimizations using the 6-31G**, 6-311++G**, and cc-pVTZ basis sets, and characterized through normal

mode analyses. Energy refinements for each point were done at the QCISD(T) level using the same three basis sets. It was shown that relative energy changes between the two levels of electron correlation were small. Structural changes for the critical points with increasing basis set were also small, and all predicted structures were in good agreement with experiment, where available. Because the geometries of HCN and *sym*-triazine are described extremely well at the MP2 level with all three basis sets, this suggests accurate geometries are available without requiring large basis sets. The MP2 frequencies show reasonable comparison with experimental values where available. Temperature-corrected (T=298 K) reaction enthalpies for dissociation of *sym*-triazine [reaction (I)], however, were lower than experiment (Ondrey and Bersohn 1984) by 18%.

IRC calculations leading from the transition state for formation/dissociation of *sym*-triazine provided mechanistic insight into these reactions. The species along the reaction path have three-fold symmetry, in agreement with photodissociation experiments that clearly show concerted triple dissociation of the *sym*-triazine (Ondrey and Bersohn 1984). The large change in the HCN angle going from the transition state to the $(HCN)_3$ cluster/HCN products could explain the experimentally observed excitation of the HCN bending vibration in the products of *sym*-triazine photodissociated at 193 nm (Goates, Chu, and Flynn 1984). The lack of excitation in the corresponding C-H and C-N bonds could be explained by the small changes in these geometric parameters along the reaction path from the transition state to the HCN products.

Since such concerted triple association/decomposition reactions are considered to be uncommon, we attempted an analysis that could show why these reactions occur, using projections of the vibrational eigenvectors of *sym*-triazine and the $(HCN)_3$ cluster onto the eigenvectors at various points along the reaction path that are associated with the direction of reaction coordinate for the concerted reactions. For points all along the reaction path, including the transition state, three vibrational modes of *sym*-triazine and two vibrational modes of the $(HCN)_3$ cluster project strongly onto the reaction path. Two of the modes that project strongly in both *sym*-triazine and the $(HCN)_3$ cluster are symmetric ring-breathing motions, while the third in *sym*-triazine is a C-H rock. Two other vibrations of the $(HCN)_3$ cluster and a vibration in *sym*-triazine also couple to portions of the reaction path, though not as strongly as the aforementioned breathing modes. These projections indicate that certain vibrational modes of *sym*-triazine and the $(HCN)_3$ cluster are coupled to the reaction coordinate, providing mechanisms through which reaction energy of the two species can transfer into the reaction path, resulting in the concerted association/decomposition reactions. The existence of the cyclic $(HCN)_3$ cluster in the reaction coordinate reduces the gross entropic effects that would hinder the concerted triple association reaction, putting the system in a preferential arrangement for concerted association if reaction energy is appropriately distributed among this cluster.

5. REFERENCES

Dunning, T. H. Jr. Journal of Chemical Physics, vol. 90, p. 1007, 1989.

Frisch, M. J., G. W. Trucks, H. B. Schlegel, P. M. W. Gill, B. G. Johnson, M. A. Robb, J. R. Cheeseman, T. Keith, G. A. Petersson, J. A. Montgomery, K. Raghavachari, M. A. Al-Laham, V. G. Zakrzewski, J. V. Ortiz, J. B. Foresman, J. Cioslowski, B. B. Stefanov, A. Nanayakkara, M. Challacombe, C. Y. Peng, P. Y. Ayala, W. Chen, M. W. Wong, J. L. Andres, E. S. Replogle, R. Gomperts, R. L. Martin, D. J. Fox, J. S. Binkley, D. J. Defrees, J. Baker, J. P. Stewart, M. Head-Gordon, C. Gonzalez, and J. A. Pople. Gaussian 94, Revision B.1, Gaussian, Inc., Pittsburgh, PA, 1995.

Goates, S. R., J. O. Chu, and G. W. Flynn. Journal of Chemical Physics, vol. 81, p. 4521, 1984.

Gordon, M. S. Chemical Physics Letters, vol. 76, p. 163, 1980.

Hariharan, P. C., and J. A. Pople. Theoretica Chimica Acta, vol. 28, p. 213, 1973.

Hehre, W. J., R. Ditchfield, and J. A. Pople. Journal of Chemical Physics, vol. 56, p. 2257, 1972.

Herzberg, G. Infrared and Raman Spectra of Polyatomic Molecules. Princeton, NJ: Van Nostrand, 1945.

Huber, K. P., and G. Herzberg. Molecular Spectra and Molecular Structure. IV. Constants of Diatomic Molecules. New York: Van Nostrand Reinhold, 1979.

Jucks, K. W., and R. E. Miller. Journal of Chemical Physics, vol. 88, p. 2196, 1988.

Kendall, R. A., T. H. Dunning, Jr., and R. J. Harrison. Journal of Chemical Physics, vol. 96, p. 6796, 1992.

King, D. S., C. T. Denny, R. M. Hochstrasser, and A. B. Smith III. Journal of the American Chemical Society, vol. 99, p. 271, 1977.

Krishnan, R., J. S. Binkley, R. Seeger, and J. A. Pople. Journal of Chemical Physics, vol. 72, p. 650, 1980.

Kurnig, I. J., H. Lischka, and A. Karpfen. Journal of Chemical Physics, vol. 92, p. 2469, 1990.

Lancaster, J. E., R. F. Stamm, and N. B. Colthup. Spectrochimica Acta. vol. 17, p. 155, 1961.

Lancaster, J. E., and B. P. Stoicheff. Canadian Journal of Physics, vol. 34, p. 1016, 1956.

McLean, A. D., and G. S. Chandler. Journal of Chemical Physics, vol. 72, p. 5639, 1980.

Migrdichian, V. The Chemistry of Organic Cyanogen Compounds. New York: Reinhold Publishing Co., p. 349, 1947.

Miller, W. H., N. C. Handy, and J. E. Adams. Journal of Chemical Physics, vol. 72, p. 99, 1980.

Ondrey, G. S., and R. Bersohn. Journal of Chemical Physics, vol. 81, p. 4517, 1984.

Rice, B. M., J. Grosh, and D. L. Thompson. Journal of Chemical Physics, vol. 102, p. 8790, 1995.

Waite, B. A., and W. H. Miller. Journal of Chemical Physics, vol. 74, p. 3910, 1981.

Woon, D. E., and T. H. Dunning, Jr. Journal of Chemical Physics, vol. 98, p. 1358, 1993.

Zhao, X., E. J. Hintsa, and Y. T. Lee. Journal of Chemical Physics, vol. 88, p. 801, 1988.

Zhao, X., W. B. Miller, E. J. Hintsa, and Y. T. Lee. Journal of Chemical Physics, vol. 90, p. 5527, 1989.

NO. OF COPIES	ORGANIZATION
2	DEFENSE TECHNICAL INFO CTR ATTN DTIC DDA 8725 JOHN J KINGMAN RD STE 0944 FT BELVOIR VA 22060-6218
1	DIRECTOR US ARMY RESEARCH LAB ATTN AMSRL OP SD TA 2800 POWDER MILL RD ADELPHI MD 20783-1145
3	DIRECTOR US ARMY RESEARCH LAB ATTN AMSRL OP SD TL 2800 POWDER MILL RD ADELPHI MD 20783-1145
1	DIRECTOR US ARMY RESEARCH LAB ATTN AMSRL OP SD TP 2800 POWDER MILL RD ADELPHI MD 20783-1145
	ABERDEEN PROVING GROUND
2	DIR USARL ATTN AMSRL OP AP L (305)

NO. OF COPIES	ORGANIZATION
1	HQDA ATTN SARD TT DR F MILTON PENTAGON WASHINGTON DC 20310-0103
1	HQDA ATTN SARD TT MR J APPEL PENTAGON WASHINGTON DC 20310-0103
1	HQDA OASA RDA ATTN DR C H CHURCH PENTAGON ROOM 3E486 WASHINGTON DC 20310-0103
4	COMMANDER US ARMY RESEARCH OFFICE ATTN R GHIRARDELLI D MANN R SINGLETON R SHAW P O BOX 12211 RSCH TRNGLE PK NC 27709-2211
1	DIRECTOR ARMY RESEARCH OFFICE ATTN AMXRO RT IP LIB SERVICES P O BOX 12211 RSCH TRNGLE PK NC 27709-2211
2	COMMANDER US ARMY ARDEC ATTN SMCAR AEE B D S DOWNS PCTNY ARSNL NJ 07806-5000
2	COMMANDER US ARMY ARDEC ATTN SMCAR AEE J A LANNON PCTNY ARSNL NJ 07806-5000
1	COMMANDER US ARMY ARDEC ATTN SMCAR AEE BR L HARRIS PCTNY ARSNL NJ 07806-5000
2	COMMANDER US ARMY MISSILE COMMAND ATTN AMSMI RD PR E A R MAYKUT AMSMI RD PR P R BETTS REDSTONE ARSENAL AL 35809

NO. OF COPIES	ORGANIZATION
1	OFFICE OF NAVAL RESEARCH DEPARTMENT OF THE NAVY ATTN R S MILLER CODE 432 800 N QUINCY STREET ARLINGTON VA 22217
1	COMMANDER NAVAL AIR SYSTEMS COMMAND ATTN J RAMNARACE AIR 54111C WASHINGTON DC 20360
2	COMMANDER NAVAL SURFACE WARFARE CENTER ATTN R BERNECKER R 13 G B WILMOT R 16 SILVER SPRING MD 20903-5000
5	COMMANDER NAVAL RESEARCH LABORATORY ATTN M C LIN J MCDONALD E ORAN J SHNUR R J DOYLE CODE 6110 WASHINGTON DC 20375
2	COMMANDER NAVAL WEAPONS CENTER ATTN T BOGGS CODE 388 T PARR CODE 3895 CHINA LAKE CA 93555-6001
1	SUPERINTENDENT NAVAL POSTGRADUATE SCHOOL DEPT OF AERONAUTICS ATTN D W NETZER MONTEREY CA 93940
3	AL LSCF ATTN R CORLEY R GEISLER J LEVINE EDWARDS AFB CA 93523-5000
1	AFOSR ATTN J M TISHKOFF BOLLING AIR FORCE BASE WASHINGTON DC 20332

NO. OF COPIES	ORGANIZATION
1	OSD SDIO IST ATTN L CAVENY PENTAGON WASHINGTON DC 20301-7100
1	COMMANDANT USAFAS ATTN ATSF TSM CN FORT SILL OK 73503-5600
1	UNIV OF DAYTON RSCH INSTITUTE ATTN D CAMPBELL AL PAP EDWARDS AFB CA 93523
1	NASA LANGLEY RESEARCH CENTER ATTN G B NORTHAM MS 168 LANGLEY STATION HAMPTON VA 23365
4	NATIONAL BUREAU OF STANDARDS US DEPARTMENT OF COMMERCE ATTN J HASTIE M JACOX T KASHIWAGI H SEMERJIAN WASHINGTON DC 20234
2	DIRECTOR LAWRENCE LIVERMORE NATIONAL LAB ATTN C WESTBROOK W TAO MS L 282 P O BOX 808 LIVERMORE CA 94550
1	DIRECTOR LOS ALAMOS NATIONAL LAB ATTN B NICHOLS T7 MS B284 P O BOX 1663 LOS ALAMOS NM 87545
2	PRINCETON COMBUSTION RESEARCH LABORATORIES INC ATTN N A MESSINA M SUMMERFIELD PRINCETON CORPORATE PLAZA BLDG IV SUITE 119 11 DEERPARK DRIVE MONMOUTH JUNCTION NJ 08852

NO. OF COPIES	ORGANIZATION
3	DIRECTOR SANDIA NATIONAL LABORATORIES DIVISION 8354 ATTN S JOHNSTON P MATTERN D STEPHENSON LIVERMORE CA 94550
1	BRIGHAM YOUNG UNIVERSITY DEPT OF CHEMICAL ENGINEERING ATTN M W BECKSTEAD PROVO UT 84058
1	CALIFORNIA INSTITUTE OF TECH JET PROPULSION LABORATORY ATTN L STRAND MS 125 224 4800 OAK GROVE DRIVE PASADENA CA 91109
1	CALIFORNIA INSTITUTE OF TECHNOLOGY ATTN F E C CULICK MC 301 46 204 KARMAN LAB PASADENA CA 91125
1	UNIVERSITY OF CALIFORNIA LOS ALAMOS SCIENTIFIC LAB P O BOX 1663 MAIL STOP B216 LOS ALAMOS NM 87545
1	UNIVERSITY OF CALIFORNIA BERKELEY CHEMISTRY DEPARMENT ATTN C BRADLEY MOORE 211 LEWIS HALL BERKELEY CA 94720
1	UNIVERSITY OF CALIFORNIA SAN DIEGO ATTN F A WILLIAMS AMES B010 LA JOLLA CA 92093
2	UNIV OF CALIFORNIA SANTA BARBARA QUANTUM INSTITUTE ATTN K SCHOFIELD M STEINBERG SANTA BARBARA CA 93106
1	UNIV OF COLORADO AT BOULDER ENGINEERING CENTER ATTN J DAILY CAMPUS BOX 427 BOULDER CO 80309-0427

NO. OF COPIES	ORGANIZATION
3	UNIV OF SOUTHERN CALIFORNIA DEPT OF CHEMISTRY ATTN R BEAUDET S BENSON C WITTIG LOS ANGELES CA 90007
1	CORNELL UNIVERSITY DEPARTMENT OF CHEMISTRY ATTN T A COOL BAKER LABORATORY ITHACA NY 14853
1	UNIVERSITY OF DELAWARE CHEMISTRY DEPARTMENT ATTN T BRILL NEWARK DE 19711
1	UNIVERSITY OF FLORIDA DEPT OF CHEMISTRY ATTN J WINEFORDNER GAINESVILLE FL 32611
3	GEORGIA INSTITUTE OF TECHNOLOGY SCHOOL OF AEROSPACE ENGINEERING ATTN E PRICE W C STRAHLE B T ZINN ATLANTA GA 30332
1	UNIVERSITY OF ILLINOIS DEPT OF MECH ENG ATTN H KRIER 144MEB 1206 W GREEN ST URBANA IL 61801
1	THE JOHNS HOPKINS UNIV CPIA ATTN T W CHRISTIAN 10630 LITTLE PATUXENT PKWY SUITE 202 COLUMBIA MD 21044-3200
1	UNIVERSITY OF MICHIGAN GAS DYNAMICS LAB ATTN G M FAETH AEROSPACE ENGINEERING BLDG ANN ARBOR MI 48109-2140
1	UNIVERSITY OF MINNESOTA DEPT OF MECHANICAL ENGINEERING ATTN E FLETCHER MINNEAPOLIS MN 55455

NO. OF COPIES	ORGANIZATION
4	PENNSYLVANIA STATE UNIVERSITY DEPT OF MECHANICAL ENGINEERING ATTN K KUO M MICCI S THYNELL V YANG UNIVERSITY PARK PA 16802
2	PRINCETON UNIVERSITY FORRESTAL CAMPUS LIBRARY ATTN K BREZINSKY I GLASSMAN P O BOX 710 PRINCETON NJ 08540
1	PURDUE UNIVERSITY SCHL OF AERONAUTICS & ASTRONAUTICS ATTN J R OSBORN GRISSOM HALL WEST LAFAYETTE IN 47906
1	PURDUE UNIVERSITY DEPARTMENT OF CHEMISTRY ATTN E GRANT WEST LAFAYETTE IN 47906
2	PURDUE UNIVERSITY SCHL OF MECHANICAL ENGNRNG ATTN N M LAURENDEAU S N B MURTHY TSPC CHAFFEE HALL WEST LAFAYETTE IN 47906
1	RENSSELAER POLYTECHNIC INST DEPT OF CHEMICAL ENGINEERING ATTN A FONTIJN TROY NY 12181
1	STANFORD UNIVERSITY DEPT OF MECHANICAL ENGINEERING ATTN R HANSON STANFORD CA 94305
1	UNIVERSITY OF TEXAS DEPT OF CHEMISTRY ATTN W GARDINER AUSTIN TX 78712
1	VA POLYTECH INST AND STATE UNIV ATTN J A SCHETZ BLACKSBURG VA 24061

NO. OF COPIES	ORGANIZATION
1	APPLIED COMBUSTION TECHNOLOGY INC ATTN A M VARNEY P O BOX 607885 ORLANDO FL 32860
2	APPLIED MECHANICS REVIEWS ASME ATTN R E WHITE & A B WENZEL 345 E 47TH STREET NEW YORK NY 10017
1	TEXTRON DEFENSE SYSTEMS ATTN A PATRICK 2385 REVERE BEACH PARKWAY EVERETT MA 02149-5900
1	BATTELLE TWSTIAC 505 KING AVENUE COLUMBUS OH 43201-2693
1	COHEN PROFESSIONAL SERVICES ATTN N S COHEN 141 CHANNING STREET REDLANDS CA 92373
1	EXXON RESEARCH & ENG CO ATTN A DEAN ROUTE 22E ANNANDALE NJ 08801
1	GENERAL APPLIED SCIENCE LABS INC 77 RAYNOR AVENUE RONKONKAMA NY 11779-6649
1	GENERAL ELECTRIC ORDNANCE SYSTEMS ATTN J MANDZY 100 PLASTICS AVENUE PITTSFIELD MA 01203
1	GENERAL MOTORS RSCH LABS PHYSICAL CHEMISTRY DEPARTMENT ATTN T SLOANE WARREN MI 48090-9055
2	HERCULES INC ATTN W B WALKUP E A YOUNT P O BOX 210 ROCKET CENTER WV 26726

NO. OF COPIES	ORGANIZATION
1	HERCULES INC ATTN R V CARTWRIGHT 100 HOWARD BLVD KENVIL NJ 07847
1	ALLIANT TECHSYSTEMS INC MARINE SYSTEMS GROUP ATTN D E BRODEN MS MN50 2000 600 2ND STREET NE HOPKINS MN 55343
1	ALLIANT TECHSYSTEMS INC ATTN R E TOMPKINS MN 11 2720 600 SECOND ST NORTH HOPKINS MN 55343
1	IBM CORPORATION RESEARCH DIVISION ATTN A C TAM 5600 COTTLE ROAD SAN JOSE CA 95193
1	IIT RESEARCH INSTITUTE ATTN R F REMALY 10 WEST 35TH STREET CHICAGO IL 60616
1	LOCKHEED MISSILES & SPACE CO ATTN GEORGE LO 3251 HANOVER STREET DEPT 52 35 B204 2 PALO ALTO CA 94304
1	OLIN ORDNANCE ATTN V MCDONALD LIBRARY P O BOX 222 ST MARKS FL 32355-0222
1	PAUL GOUGH ASSOCIATES INC ATTN P S GOUGH 1048 SOUTH STREET PORTSMOUTH NH 03801-5423
1	HUGHES AIRCRAFT COMPANY ATTN T E WARD PO BOX 11337 TUCSON AZ 85734-1337

NO. OF COPIES	ORGANIZATION
1	SCIENCE APPLICATIONS INC ATTN R B EDELMAN 23146 CUMORAH CREST WOODLAND HILLS CA 91364
3	SRI INTERNATIONAL ATTN G SMITH D CROSLEY D GOLDEN 333 RAVENSWOOD AVENUE MENLO PARK CA 94025
1	STEVENS INSTITUTE OF TECH DAVIDSON LABORATORY ATTN R MCALEVY III HOBOKEN NJ 07030
1	SVERDRUP TECHNOLOGY INC LERC GROUP ATTN R J LOCKE MS SVR 2 2001 AEROSPACE PARKWAY BROOK PARK OH 44142
1	SVERDRUP TECHNOLOGY INC ATTN J DEUR 2001 AEROSPACE PARKWAY BROOK PARK OH 44142
3	THIOKOL CORPORATION ELKTON DIVISION ATTN R BIDDLE R WILLER TECH LIB P O BOX 241 ELKTON MD 21921
3	THIOKOL CORPORATION WASATCH DIVISION ATTN S J BENNETT P O BOX 524 BRIGHAM CITY UT 84302
1	UNITED TECHNOLOGIES RSCH CENTER ATTN A C ECKBRETH EAST HARTFORD CT 06108
1	UNITED TECHNOLOGIES CORP CHEMICAL SYSTEMS DIVISION ATTN R R MILLER P O BOX 49028 SAN JOSE CA 95161-9028

NO. OF COPIES	ORGANIZATION
1	UNIVERSAL PROPULSION COMPANY ATTN H J MCSPADDEN 25401 NORTH CENTRAL AVENUE PHOENIX AZ 85027-7837
1	VERITAY TECHNOLOGY INC ATTN E B FISHER 4845 MILLERSPORT HIGHWAY EAST AMHERST NY 14051-0305
1	FREEDMAN ASSOCIATES ATTN E FREEDMAN 2411 DIANA ROAD BALTIMORE MD 21209-1525
3	ALLIANT TECHSYSTEMS ATTN C CANDLAND L OSGOOD R BECKER 600 SECOND ST NE HOPKINS MN 55343
1	DIRECTOR US ARMY BENET LABS ATTN AMSTA AR CCB T SAM SOPOK WATERVLIET NY 12189

NO. OF
COPIES ORGANIZATION

ABERDEEN PROVING GROUND

36 DIR USARL
ATTN: AMSRL-WT-P, A HORST
AMSRL-WT-PC,
R A FIFER
G F ADAMS
W R ANDERSON
R A BEYER
S W BUNTE
C F CHABALOWSKI
K P MCNEILL-BOONSTOPPEL
A COHEN
R CUMPTON
R DANIEL
D DEVYNCK
N F FELL
B E FORCH
J M HEIMERL
A J KOTLAR
M R MANAA
W F MCBRATNEY
K L MCNESBY
S V MEDLIN
M S MILLER
A W MIZIOLEK
S H MODIANO
J B MORRIS
J E NEWBERRY
S A NEWTON
R A PESCE-RODRIGUEZ
B M RICE
R C SAUSA
M A SCHROEDER
J A VANDERHOFF
M WENSING
A WHREN
J M WIDDER
C WILLIAMSON
AMSRL-CI-CA, R PATEL

INTENTIONALLY LEFT BLANK.

USER EVALUATION SHEET/CHANGE OF ADDRESS

This Laboratory undertakes a continuing effort to improve the quality of the reports it publishes. Your comments/answers to the items/questions below will aid us in our efforts.

1. ARL Report Number/Author ARL-TR-1096 (Pai) Date of Report June 1996

2. Date Report Received _____

3. Does this report satisfy a need? (Comment on purpose, related project, or other area of interest for which the report will be used.) _____

4. Specifically, how is the report being used? (Information source, design data, procedure, source of ideas, etc.) _____

5. Has the information in this report led to any quantitative savings as far as man-hours or dollars saved, operating costs avoided, or efficiencies achieved, etc? If so, please elaborate. _____

6. General Comments. What do you think should be changed to improve future reports? (Indicate changes to organization, technical content, format, etc.) _____

CURRENT ADDRESS

Organization

Name

Street or P.O. Box No.

City, State, Zip Code

7. If indicating a Change of Address or Address Correction, please provide the Current or Correct address above and the Old or Incorrect address below.

OLD ADDRESS

Organization

Name

Street or P.O. Box No.

City, State, Zip Code

(Remove this sheet, fold as indicated, tape closed, and mail.)
(DO NOT STAPLE)

DEPARTMENT OF THE ARMY

OFFICIAL BUSINESS

NO POSTAGE
NECESSARY
IF MAILED
IN THE
UNITED STATES

BUSINESS REPLY MAIL
FIRST CLASS PERMIT NO 0001,APG,MD

POSTAGE WILL BE PAID BY ADDRESSEE

DIRECTOR
U.S. ARMY RESEARCH LABORATORY
ATTN: AMSRL-WT-PC
ABERDEEN PROVING GROUND, MD 21005-5066